frontiers in Pharmacology

# Tan IIA suppresses proliferation and Inflammatory Cytokine Production of Synovial Fibroblasts from Rheumatoid Arthritis Patients Induced by TNF-a and attenuates the inflammatory response in AIA mice

Ligang Jie[1*], Hongyan Du[2*], Yuechun Wang[1], Yongchang Zeng[2], Xiaoming Huang[2], Dingfei Liu[2], Lvlan Ye[2], Yang Li[2], Xiaochen Chen[2], Tiancai Liu[2], Hongwei Li[2], Jing Wu[1], Qinghong Yu[1], Yingsong Wu[2]

[1]Zhujiang Hospital, Southern Medical University, China, [2]Southern Medical University, China

*Submitted to Journal:*
Frontiers in Pharmacology

*Specialty Section:*
Ethnopharmacology

*ISSN:*
1663-9812

*Article type:*
Original Research Article

*Received on:*
05 Feb 2020

*Accepted on:*
14 Apr 2020

*Provisional PDF published on:*
14 Apr 2020

*Frontiers website link:*
www.frontiersin.org

*Citation:*
Jie L, Du H, Wang Y, Zeng Y, Huang X, Liu D, Ye L, Li Y, Chen X, Liu T, Li H, Wu J, Yu Q and Wu Y(2020) Tan IIA suppresses proliferation and Inflammatory Cytokine Production of Synovial Fibroblasts from Rheumatoid Arthritis Patients Induced by TNF-α and attenuates the inflammatory response in AIA mice. *Front. Pharmacol.* 11:568. doi:10.3389/fphar.2020.00568

# Tan IIA Suppresses Proliferation and Inflammatory Cytokine Production of Synovial Fibroblasts from Rheumatoid Arthritis Patients Induced by TNF-α and Attenuates the Inflammatory Response in AIA Mice

Hongyan Du[1], Yuechun Wang[2,3], Yongchang Zeng[1], Xiaoming Huang[1], Dingfei Liu[1], Lvlan Ye[1], Yang Li[1], Xiaochen Chen[1,3], Tiancai Liu[1], Hongwei Li[1], Jing Wu[2], Qinghong Yu[2], Yingsong Wu[1#], Ligang Jie[2#]

[1]School of Laboratory Medicine and Biotechnology, Southern Medical University, Guangzhou, Guangdong, China; [2] Department of Rheumatology and Clinical Immunology, Zhujiang Hospital, Southern Medical University, Guangzhou, Guangdong, China; [3]School of Chinses Medicine, Southern Medical University, Guangzhou, Guangdong, China

[#]**Correspondence:**

**Yingsong Wu**, Ph.D.,

School of Laboratory Medicine and Biotechnology, Southern Medical University, 1023 South Shatai Road, Guangzhou, Guangdong 510515, China.

E-mail: wg@smu.edu.cn

**Ligang Jie,** M.D., Ph.D.,

Department of Rheumatology and Clinical Immunology, Zhu Jiang Hospital, Southern Medical University, 253 Gongye Ave, Guangzhou, Guangdong 510282, China.

E-mail: Jieligang@hotmail.com

Running Title : Tan IIA suppresses RA-FLSs and ameliorates AIA severity

Rheumatoid arthritis (RA) is a chronic and progressive autoimmune disease, in which activated RA fibroblast-1ike synoviocytes (RA-FLSs) are one of the main responsible for inducing morbidity. Previous reports have shown that RA-FLSs have proliferative features similar to cancer cells, in addition to causing cartilage erosion that eventually causes joint damage. Thus, new therapeutic strategies and drugs, which can effectively contain the abnormal hyperplasia of RA-FLSs and restrain RA development, are necessary for the treatment of RA. Tanshinone IIA (Tan IIA), one of the main phytochemicals isolated from *Salvia miltiorrhiza*, is capable of promoting RA-FLSs apoptosis and inhibiting arthritis in AIA mice model. In addition, RA patients treated at our clinic with Tan IIA showed significant improvements in their clinical symptoms. However, the detailed molecular mechanism of the Tan IIA effect in RA is unknown. To clarify this mechanism, we evaluated the antiproliferative and inhibitory effects of proinflammatory factors production caused by Tan IIA on RA-FLSs. We demonstrated that Tan IIA can restrict the proliferation, migration and invasion of RA-FLSs in time and dose dependent manner. Moreover, Tan IIA effectively suppressed the increase in mRNA expression of some matrix metalloproteinases and proinflammatory factors induced by TNF-α in RA-FLSs, resulting in inflammatory reactivity inhibition and in blocking the destruction of the knee joint. Trough the integration of the network pharmacology analyzes with the experimental data obtained, it is revealed that effects of Tan IIA on RA can be attributed to its influence on different signaling pathways, including MAPK, AKT/mTOR, HIF-1 and NF-kB. Taken together, these data suggest that the compound Tan IIA has great therapeutic potential for RA treatment.

**Key words**: Tan IIA; suppress; RA-FLSs; AIA; MAPK; AKT/mTOR; HIF-1α

## INTRUDUCTION

Rheumatoid arthritis (RA) is a chronic and systemic autoimmune disease characterized by deformity and joint dysfunction (Smolen and Aletaha et al., 2016). Although the pathogenesis and etiology of RA have not been fully explained, fibroblast-like synoviocytes (FLSs) are considered crucial in the synovial hyperplasia development and in the progressive joint destruction in RA patients (Huber and Distler et al., 2006; Lefevre and Knedla et al., 2009). Recent evidence indicates that activated of RA-FLSs display biological characteristics similar to tumor cells, such as aggressive proliferation, migration, and invasion. Remarkably, these features are conducive to causing damage to articular cartilage and bone (Bustamante and Garcia-Carbonell et al., 2017; Wang and Li et al., 2019; Wang and Zhao, 2019). Therefore, the inactivation of RA-FLSs is pointed out as a potential therapeutic strategy for the treatment of RA.

Many natural ingredients from herbal medicine have been found to be pharmaceutically effective against RA. *Salvia miltiorrhiza*, one of famous herbal medicines, has been widely used to treat cardiovascular diseases in China. Tanshinone IIA (Tan IIA) is the main phytochemical isolated from *Salvia miltiorrhiza* and is the main responsible for its beneficial cardiovascular effect. Besides, several studies have revealed other medicinal effects of Tan IIA, including anti-tumor, anti-proliferation and anti-inflammatory effects in various cancers, such as non-small-cell lung cancer, liver cancer, cervical cancer, colorectal cancer and gastric cancer (Sui and Zhao et al., 2017; Zhang and Guo et al., 2018; Liu and Zhu et al., 2019; Wang and Luo et al., 2019; Zhang and Lin et al., 2019). Additionally, there are also reports Tan IIA could be used to treat arthritis (Jia and Zhang et al., 2017; Zhang and Huang et al., 2017).

RA patients have an increased mortality rate due to cardiovascular events. The increase in inflammation associated with RA is the main mechanism that leads to an increase in the cardiovascular mortality rate. These data may suggest that aggressive

treatment of inflammation may decrease cardiovascular risk in patients with RA. Tan IIA has been shown to have anti-inflammatory and immunomodulatory effects on atherosclerosis (Chen and Xu, 2014). Recent studies pointed out that Tan IIA can be used to antiatherosclerosis treatment targeting immune cells, antigens, cytokines, and cell signaling pathways (Ren and Fu et al., 2019). In this context, anti-inflammatory and immunomodulatory effects of Tan IIA can be used in the treatment of rheumatoid arthritis also. In fact, patients with RA treated at our clinic with compound salvia injection, in which Tan IIA is one of the main ingredients, showed significant improvements in their clinical symptoms (Jie and Huang et al., 2002; Jie and Huang et al., 2010) .

All of which indicated Tan IIA was safe and could be a potential clinical medicine, but more further research on mechanism was need for providing bases for clinical use. Especially, for the RA patients with cardiovascular disease or related risk factors, Tan IIA may be a better choice. In recent years, several studies have focused on the effect and the mechanism of tanshinone in the treatment of RA. Our previous studies demonstrated that Tan IIA induced apoptosis of RA-FLSs by blocking the cell cycle in the G2/M phase and regulating a mitochondrial pathway. In addition, other studies have shown that Tan IIA and a derivate, sodium tanshinone IIA sulfonate, inhibited proliferation, migration, invasion and inflammation in RA-FLSs and attenuated RA progression in collagen-induced arthritis (CIA) mice (Tang and Zhou et al., 2019; Wang and Li et al., 2019). However, the detailed molecular mechanisms that clarify the effect of Tan IIA on RA have not been yet discovered due to its various effects and targets. Therefore, in this study, several approaches (AIA animal model for in vivo experiment, RA-FLS strains construction for in vitro evaluating and network pharmacology and signaling pathways analyzes) were applied to further investigate the effects and therapeutic approaches of Tan IIA on RA.

## MATERIALS AND METHODS

## Animals

Male C57BL/6 mice at an age of 10–12 weeks were obtained from the Lab Animal Center of Southern Medicine University. The experiment was approved by The Southern Medical University Ethics Committee for Animal Laboratory Research. All animal experimental procedures were in accordance with the ethical guide for institutional animal care and use of Laboratory Animals of the National Institutes of Health. The mice were fed in right environment according to the previous condition (Du and Zhang et al., 2019).

## AIA induction and Tan IIA treatments

Eighteen male C57BL/6 mice with about 20g/body weigh each were divided into three groups randomly. They are normal group, AIA model group and AIA model with Tan IIA treatment group. The protocol of inducting AIA model was refer to previously described (Atkinson and Nansen, 2017; Dong and Wu et al., 2019; Du and Zhang et al., 2019; Grotsch and Bozec et al., 2019) and adjusted in some points. The experimental timeline for AIA was shown in Figure 1. Briefly, mixtures (1:1/volume ratio) of 5% bovine serum albumin (BSA, Sigma, USA) and Freund's complete adjuvant (CFA) (Sigma-Aldrich, USA) were made by emulsified. On day 0 the mice immunizations were operated by 100μL emulgator subcutaneously injecting into the knee joint space under general anesthesia. Mice were injected with 20μL emulgator in which Freund's incomplete adjuvant (IFA) (Sigma-Aldrich, USA) substituted for CFA on day 21. From day 2 to day 31 after immunized, mice were Intragastric administrated with100μL Tan IIA (30mg/kg, Selleck, Shanghai, China) every single day. Normal and AIA model groups were given an equal volume of 1% sodium carboxylmethyl cellulose suspension i.g. simultaneously. Body weight and the mediolateral knee joint diameter were monitored by ones who were blinded to the experimental design every 5 days (Frey and Huckel et al., 2018; Dong and Wu et al., 2019; Du and Zhang et al., 2019).

## Measurement of serum proinflammatory cytokines concentration

On day 40, 48, 56, and 80 after immunization, 200-300μL blood samples were gathered from the eyeballs of mice and 100-200μL serum samples were separated by centrifuge and stored at -80℃ for analysis. The ELISA detections of IL-6, IL-17 and TNF-α were carried on with ELISA Kits (Jiangsu Meimian Industrial Co., Ltd, Jiangsu, China) according to the manufacturer's instructions (Ting and Hongyan et al., 2017; Gou and Zeng et al., 2018; Du and Zhang et al., 2019).

## Measurement of spleen and liver indices

On day 80 after immunization all the mice were sacrificed by cervical dislocation. The liver and spleen indices were determinated by the ratio of spleen and liver wet weight to mice body weight (g/g), respectively. They were expressed as organ index=organ wet weight (g)/animal body weight (g) × 100% (Hu and Hepburn et al., 2005; Gou and Zeng et al., 2018; Du and Zhang et al., 2019).

## Histopathological evaluation of joints

Hind limbs with knee articular were removed from mice and fixed in Roles-Bio® Universal Tissue Fixative (Roles-Bio, Guangzhou Routh Biotechnology Co., Ltd.). Whereafter, the tissues were decalcified with Roles-Bio® Quick Decalcifying Solution (Roles-Bio, Guangzhou Routh Biotechnology Co., Ltd.) and embedded in paraffin. About 5μm paraffin sections were made and stained with hematoxylin and eosin (H&E)(Gou and Zeng et al., 2018; Du and Zhang et al., 2019). The HE results were graded in a blinded manner according to previous research (Du and Zhang et al., 2019; Grotsch and Bozec et al., 2019). The scoring standard was as follows: 1=mild, 2=moderate, and 3=severe.

## Cells isolation and culture

The synovial tissues were removed from the knee joints of active RA patients who were undergoing synovectomy with arthroscopy. The detailed data from patients who were 2 males and 4 females were shown in Table S1. RA patients selected into our research conformed to the American College of Rheumatology revised criteria of the diagnosis of RA (Arnett and Edworthy et al., 1988) and were informed consent. Moreover, our experiments were under control with the guideline formulated by the Medical Ethics Committee of the Zhujiang Hospital, Southern Medical University and were operated according to the recommendations of the Declaration of Helsinki. The primary synoviocytes (RA-FLSs) were isolated from the harvested synovial tissue and cultured according to our previous published research (Du and Zhang et al., 2019). After subcultured the three to six passage RA-FLSs were used for the following experiments. All reagents for culturing cells were purchased from Gibco® (Thermo Fisher Scientific, MA, USA).

**Cell Viability Assay**

RA-FLSs were planted into a 96-well plate and treated with Tan IIA ($C_{19}H_{18}O_3$, ≥98% HPLC, CAS:568-72-9, Selleck) at various concentration（0μM, 2.5μM, 5μM, 10μM, 20μM）and TNF-α(20ng/mL). The cell viability assay was carried on with Cell Counting Kit (CCK-8) (KeyGEN BioTECH) according to the manufacture's instruction. The absorbance was measured at 450nm with a microplate reader.

**Cell Migration and invasion Assay**

RA-FLSs migration and invasion assay were operated by Boyden chamber with 6.5mm diameter inserts containing 8μm pores (Costar, New York, NY, USA) or coated with Matrigel basement membrane matrix (BD Biosciences, Oxford, UK) in 24-well plate. Briefly, after treated with various concentrations Tan IIA for 24 h respectively, $4\times10^3$/200μL RA-FLSs suspended in serum-free DMEM medium were

added into the upper chamber and 500μL DMEM media with 10% FBS were placed in lower well as chemoattractant. Followed by incubated, the migrating cells through the filter were fixed and stained with 0.1% crystal violet. The cells were quantified by counting the stained cells with a microscope. The mean number of cells per 5-6 random fields was calculated for each assay (Du and Zhang et al., 2019; Wu and Li et al., 2019).

**Wound Healing Assay**

RA-FLSs were planted into a 12-well culture dishes at first day. Next day a pipette tip made the scratch and deciduous cells were washed with PBS twice to remove. After treated with various concentration Tan IIA for 48hs, the wound areas were photographed with microscope and counted with software Image J. The data were shown as the mean ± SD of three independent experiments.

**RNA Isolation and Real-time PCR Assay**

Real-time PCR was performed for analyzing some cytokines and MMPs expression in RA-FLSs treated with Tan IIA according to previously described (Jie and Huang et al., 2015; Du and Zhang et al., 2019). Total RNAs in RA-FLSs treated with or without TNF-α(20ng/mL) and Tan IIA were isolated by TRIzol (Invitrogen, U.S.A.) and reverse transcribed into cDNA using the Prime Script RT Reagent kit (Takara Biotechnology, Dalian, China) referencing the manufacturer's protocol. According to the manufacturer's instructions PCR quantification for cytokines and MMPs mRNAs with SYBR Premix Ex TaqTM kit (Takara Biotechnology, Dalian, China) was carried out in an ABI 7500 type PCR instrument (Applied Biosystems Inc., Foster City, CA, USA). Dd$H_2O$ containing no template was set as negative control. All the primers were synthesized by IGE Biotech. Co., Ltd (Guangzhou, China) and listed in supplementary material Table S2. All experiments were performed in triplicate and repeated three times independently. To quantify the relative expression of each gene,

ΔΔCt method ($\Delta\Delta Ct = \Delta Ct_{sample} - \Delta Ct_{control}$) was used to indicate the ratio of the expression of the target gene in the model group to that of the control group (Du and Zhang et al., 2019; Wu and Li et al., 2019).

**Western Blot Assay**

After treated with TNF-α (20ng/mL) or/and 10μM and 20μM Tan IIA for 24h RA-FLSs were collected and extracted total protein using RIPA lysis buffer and phosphatase inhibitors (Beyotime Biotechnolgoy, Nantong, China) on ice. The proteins from RA-FLSs were obtained through separating supernatants and debris with centrifugation at 12,000 rpm for 20 min at 4 ℃. The Pierce® BCA Protein Assay Kit (Thermo Scientific, USA) was used to the protein concentration. The levels of protein were adjusted to 0.5–1 μg/μL and detected by Automated electrophoresis western analysis assay (ProteinSimple, Biotechne, San Jose CA, United States) as described previously (Baradaran-Heravi and Balgi et al., 2016). According to the user manual, all procedures were performed using the manufacturer's reagents. Briefly, 8 μl diluted protein lysate was mixed with 2μl of 5× fluorescent master mix and heated at 95◦C for 5 min. Various ingredients, including sample (about 1μg), blocking reagent, wash buffer, primary antibodies, secondary antibodies, and chemiluminescent substrate were alloted into the designated wells in a manufacturer-provided microplate. The plate was loaded into the instrument, and protein was drawn into individual capillaries on a 25-capillary cassette provided by the manufacturer (Jess/Wes Seperation 12-230kDa 8×25 Capillary Cartridges kit). Protein separation and immunodetection were automatically performed on the individual capillaries using the default settings. The data was analyzed with inbuilt Compass software (ProteinSimple, Biotechne, United States). The truncated and target protein peak intensities (area under the curve) were normalized to that of the vinculin peak, used as a loading control. Primary antibodies included AKT, mTOR, p70S6K, 4E-BP1, p38 MAPK, p44/42 MAPK (Erk1/2), JNK, NFκB p65, Iκκα, HIF-1α and their corresponding phosphorylation antibody, Phospho-Akt (Ser473), Phospho-p70 S6

Kinase (Thr389), Phospho-4E-BP1 (Ser65), Phospho-p38 MAPK(Thr180/Tyr182) , Phospho-p44/42 MAPK (Erk1/2) (Thr202/Tyr204), Phospho-JNK (Thr183/Tyr185), p-NFκB p65(Ser 536) and p-Iκκα/β(Ser176/180), which were all purchased from Cell Signaling Technology, USA. GAPDH antibodies as reference standard for quantification were purchased from bioworld technology. Inc.

**Measurements of Cytokines Level by ELISA**

To determine the effect of Tan IIA on cytokines production the ELISA experiments were operated using human enzyme-linked immunosorbent assay (ELISA) kits (Jiangsu Meimian Industrial Co., Ltd, Jiangsu, China) according to the manufacturer's instructions. For example, RA-FLSs were seeded into 6-well plates and treated with TNF-α (20ng/mL) or/and 10μM and 20μM Tan IIA for 48h. The culture supernatants were collected and IL-6 level releasing from RA-FLSs was detected as previously described (Jie and Huang et al., 2015; Du and Zhang et al., 2019). By the same method other Cytokines assays were carried on. All experiments were manipulated in triplicate and replicated 3 times.

**Searching the Tan IIA potential targets in RA by network pharmacology**

Firstly, data preparation was carried on by searching Rheumatoid Arthritis-related genes at the National Biotechnology Center (https://www.ncbi.nlm.nih.gov). Additionally, the chemical structure, molecular weight, 2D structure, 3D structure, chemical number and physicochemical properties of Tan IIA had to be confirmed. The target genes of Tan IIA were obtained by Pharmmapper (http://www.lilab-ecust.cn/pharmmapper/). Next, drug-target-disease interaction network was constructed. Based on the functions of the human genes related to rheumatoid arthritis and the potential Tan IIA targets the Venn diagram was designed and the intersection target genes were obtained. Moreover, The protein-protein interaction network （PPI）was constructed on-line by STRING (https://string-db.org/cgi/input.pl).

Finally, Biological process and pathway analysis was operated. According to the function of human genes related to rheumatoid arthritis and potential Tan IIA targets, the bioconductor database were used for performing Gene Ontology (GO) Enrichment and Kyoto Encyclopedia of Genes and Genomes (KEGG) pathway enrichment analysis of target genes through R (R 3.6.1 for Windows). The target genes were screened with $P < 0.05$ as the critical value of significant functions and pathways, and the main signaling pathways and biological processes involved in the pharmacological effects of Tan IIA in treating rheumatoid arthritis were obtained.

**Statistical Analysis**

Data from multiple experiments were presented as the mean ± standard deviation (SD). Statistical software was used for all data analysis. The statistical difference comparisons (P-values) between two groups were calculated using Student's t-test and P-values between more than three groups were calculated using one-way analysis of variance (ANOVA) with GraphPad Prism 8.0. Two-sided $p<0.05$ was considered statistically significant. Number of replicates and/or total number of animals were shown in figure legends or within the figures.

## RESULTS

### Tan IIA attenuates the inflammatory response in mice with AIA

### Tan IIA suppresses the weight loss and knee joint swell on AIA mice

All the mice from different groups could get food and water freely during the whole study period. To make clear the effect of Tan IIA on AIA model mice, the mean changes in body weight of mice were monitored every 5 days from day 0 to day 80. It was shown in Fig. 2A that the mean body weight change of mice from AIA group significantly appeared decrease comparing with the change from normal group at the $25^{th}$ day after immunization. Nevertheless, compared with normal group the mean body weight change of mice from the group treated with Tan IIA (30mg/kg) via gavage was little decline at that time. There was significant difference between Tan IIA treatment group and AIA model group.

Synchronously, the effect of Tan IIA on arthritis severity characterized with measurements of the knee joint diameters were assessed every 5 days. As shown in Fig. 2B, the mean value of diameters for knee joints from AIA mice increased obviously comparing to normal group from $20^{th}$ day after immunization because of obvious swelling. Moreover, the increase was rapid from $25^{th}$ day to $40^{th}$ day, which was up to peak value. After $40^{th}$ day the mean value of diameters gradually came down. The values of mean diameters during whole process were significantly different from that of the normal control group. However, comparing with AIA mice the mean value of diameters for knee joints from the mice with Tan IIA treatment was less from the $25^{th}$ to $60^{th}$ day.

### Tan IIA reduces spleen and liver indices of AIA mice

The spleen and liver indices from mice in different groups were assessed for evaluating the Tan IIA effect on main immune organs. The spleen and liver indices from mice of AIA model group obviously raised comparing with the data from

normal group (Fig.2C). Nevertheless, the spleen and liver indices from Tan IIA treatment group were significantly less than the ones from AIA group.

**Tan IIA improves the pathohistological characters of knee joints and arthritis severity in AIA mice**

To study how Tan IIA affecting the pathohistological features of AIA mice, the histological examination of tissue sections were performed. The knee joints from all mice were removed at the 80$^{th}$ day after euthanized, followed by stained with H&E for pathohistological sections. It shown that clear and complete histological architecture through microscopic observation of the knee joint from normal control group. However, the knee joints from AIA model group appeared abnormal histological architecture, which were characterized with synovial tissue hyperplasia, massive inflammatory cells infiltration, accompanied by epithelial cell degradation and angiogenesis (microvessel density increase). Comparing with AIA group the histological architectures of knee joints from Tan IIA treatment group were mild with less synovial hyperplasia, inflammatory cells infiltration and synovial tissues erosion (Fig.2D). Additionally, as shown in Fig. 2E, the pathohistological score appeared similar tendency in three experiment groups, which suggested that Tan IIA did attenuates the inflammatory response in mice from AIA group and had a good effect of anti-arthritis.

**Tan IIA restrains proinflammatory cytokines expression in AIA mice**

On the day 40,48,56 and 80 after immunized the expressions of IL-6, IL-17, and TNF-α in serum from AIA mice with and without Tan IIA treatment were examined by ELISA for exploring how the Tan IIA affecting the proinflammatory cytokines. As for IL-6, its expression in serum from AIA mice were significantly higher than ones from normal control group at 40$^{th}$, 48$^{th}$, and 56$^{th}$ day. Moreover, it was obviously increased comparing to quantity in mice treated with Tan IIA on day 40 and 48 either. However, on day 56 and 80 there was no obviously difference

between them. Next, the similar trends on day 40, 48 and 56 were observed in IL-17 and TNF-α expression in three groups. Although there was difference occurred between normal mice and AIA mice group on day 80, no differences in IL-17 and TNF-α were witnessed between Tan IIA treatment group and AIA group (Fig.2F). All the data indicated Tan IIA (30mg/kg) could suppress production of the proinflammatory cytokines, IL-6, IL-17 and TNF-α in serum of AIA mice.

**Tan IIA suppresses the migration and invasion of RA-FLSs**

Primary RA-FLSs were separated synovial tissue from clinical samples. The Transwell experiments were operated using the transwell Boyden chamber with or without Matrigel matrix to evaluate the effect of Tan IIA on migration and invasion of RA-FLSs in vitro. 10μM and 20μM Tan IIA treatment profoundly declined both migratory and invasion ability of RA-FLSs comparing with control as presented in Fig. 3A and 3B. This result was further confirmed by wound closure assay, which shown in Fig. 3C. After 48hrs, the control group cells almost recovered the scratch place. The cells treated with Tan IIA were inhibited wound healing. Although 5μM Tan IIA did not significantly interfere with the capacity of RA-FLSs migrating from one side of wound to the other, higher concentration Tan IIA (10 and 20μM) did restrain the cell migrating into the wounded area as presented in Fig.3C. All the data indicated Tan IIA could block the migration and invasion of RA-FLSs in vitro.

**Tan IIA inhibits the viability of RA-FLSs activated by TNF-α**

As well known TNF-α is one of important pro-inflammatory cytokines conducing to RA-FLSs surviving and progressive arthritis in RA pathology(Bottini and Firestein, 2013; Bustamante and Garcia-Carbonell et al., 2017). To discover the effect of Tan IIA on the viability of RA-FLSs induced by TNF-α, the effect of Tan IIA with serial concentrations (0, 2.5, 5, 10 and 20μM) on the viability of RA-FLSs activated with TNF-α was measured. 20ng/mL TNF-α obviously promoted the viability of RA-FLSs (Fig.4A). Tan IIA almost did not affect cell viability induced by

TNF-α after 24h treatment (data not shown), while higher concentrations Tan IIA (10 and 20μM) showed a dose-dependent inhibition in cell viability induced by TNF-α after 48h treatment (Fig. 4A).

**Tan IIA suppresses the pro-inflammatory cytokines and MMPs expression stimulated by TNF-α**

Accumulating evidence pointed out that during the development of RA there were some main pro-inflammatory cytokines and matrix metalloproteinases (MMPs) contributing pathogenic factors for proliferation, migration and invasion of RA-FLSs and even erosion of cartilago articularis(Bottini and Firestein, 2013; Bustamante and Garcia-Carbonell et al., 2017). To explore the role of Tan IIA on key pro-inflammatory cytokines expression induced by TNF-α, the mRNA expression levels of *IL-6, IL-8, IL-17*, and *IL-1β,* stimulated by TNF-α in RA-FLSs treated with 10μM and 20μM Tan IIA for 24h were assessed with qPCR. As presented in Fig. 4B, although there were up-regulation more or less for mRNA level of *IL-6, IL-1β,* and *IL-8*in RA-FLSs induced by TNF-α(20ng/mL), 20μM Tan IIA did inhibit *IL-6, IL-1β* and *IL- 8* mRNA up-regulation stimulated by 20ng/mL TNF-α and 10μM Tan IIA had no obvious effect except for *IL-1β.* Unlike our expection, neither Tan IIA treatment nor TNF-α stimulating profoundly changed *IL-17* mRNA expression. Additionally, as shown in Fig. 4C, only *MMP-2* mRNA expression was increased induced by TNF-α (20ng/mL) and *MMP-3* mRNA expression was decreased by 10μM Tan IIA treatment. However, the mRNA expression of *MMP-2, MMP-3, MMP-8* and *MMP-9* significantly dropped after 20μM Tan IIA treatment, which suggested Tan IIA significantly blocked up-regulation in mRNA expression of *MMP-2, MMP-3, MMP-8* and *MMP-9* stimulated by TNF-α in RA-FLSs.

In addition, the effect of Tan IIA on some pro-inflammatory cytokines release stimulated by TNF-α was also discovered except for mRNA level. After treated with Tan IIA (10μM and 20μM) for 48hrs, ELISA assays for IL-6, IL-1β and IL- 8 in cells culture supernatant were performed. It was indicated in Fig.4D 20ng/mL TNF-α

significantly increased the IL-6 and IL-1β production in RA-FLSs, but Tan IIA treatment could suppress the increase as shown in Fig. 4D-a and Fig. 4D-b. Of interest, 20ng/mL TNF-αstimulation did not arouse profound up-regulation of IL-8, but 20μM Tan IIA indeed down-regulated IL-8 release (Fig. 4D-c). There was no detectable IL-17 in the ELISA- assay because of the less expression in cell culture supernatants. In short, the results suggest that Tan IIA may be helpful for reducing production and release of some MMPs and pro-inflammatory cytokines from RA-FLSs.

**Potential targets for Tan IIA in RA searching by database tools**

To uncover potential targets for Tan IIA in RA we searched NCBI database and obtained 1147 human genes associated with rheumatoid arthritis. At the same time, we found 297 target genes involved in Tan IIA from Pubchem and Pharmmapper database. The Venn diagram by R(R 3.6.1 for Windows) was made based on the 297 drug targets of Tan IIA and 1147 gene targets of rheumatoid arthritis (Fig.5A). We got 31 common targets, which were obtained as the key targets of tanshinone IIA in the treatment of RA. Import the common target into STRING to build the PPI network (Fig. 5B). This network consists of 71 nodes. The size of the node in the figure was formed by the size of the Degree value. The higher the Degree value, the larger the node. We predicted that the following proteins, BCL2L1, MAPK14, CTNNB1, TP53, EIF4EBP1, HIF1a, HMGB and mTOR, would be potential direct targets of Tan IIA in the treatment of rheumatoid arthritis.

Meanwhile, considering the common targets of RA and Tan IIA, there are 43 biological processes ($P<0.05$) screened by GO, including protein heterodimerization activity; growth factor activity; receptor regulator activity; disordered domain specific binding; ribonucleoprotein complex binding; receptor ligand activity, etc. Next, we performed functional enrichment analysis using the KEGG database to make clear the functions of these target genes and signaling pathways. Of note, the data shown that

the potential target genes we found were functionally related with various signal transduction pathways, including PI3K-Akt signaling pathway; Proteoglycans in cancer; Pancreatic cancer; Kaposi sarcoma-associated herpesvirus infection; Human cytomegalovirus infection; MAPK signaling pathway; Choline metabolism in cancer; hypoxia-inducible factor (HIF-1) signaling pathway(Fig. 5C). In generally, Tan IIA maybe participate in these pathways, which could ultimately affect the progression of the disease.

**Tan IIA affects the activation of RA-FLSs induced by TNF-α through modulation of MAPK, Akt/mTOR and HIF-1 pathways**

Combining results from GO and KEGG with our preliminary research data we speculated Tan IIA affected RA probably through the PI3K-Akt, MAPK and HIF-1 signaling pathway. We detected the main proteins expression and phosphorylation levesl of MAPK signal pathway, including p38MAPK, JNK and ERK to further verify our supposition the effect of Tan IIA on MAPK. After treated with 20ng/mL TNF-α and Tan IIA (10 and 20μM) for 24h, the RA-FLSs were collected and the expression and phosphorylated levels of p38MAPK, JNK, ERK were evaluated by western blot analysis. As presented in Fig.6A, enhanced p38MAPK and JNK phosphorylated activations induced by TNF-α were observed in RA-FLSs compared with control without TNF-α stimulation. Also, Tan IIA efficiently inhibited TNF-α-induced phosphorylation of p38MAPK and JNK. Intriguingly, Tan IIA had less influence on ERK phosphorylated level. The fact that Tan IIA strongly reduced p38MAPK and JNK activity may be contribute to control synovial abnormal hyperplasia in articular cavity.

Moreover, the phosphorylation level of Akt/mTOR signaling pathway and its downstream molecules in RA-FLSs, p70 ribosomal S6 kinase (p70S6K) and eukaryotic translation initiation factor 4E-binding protein 1 (4E-BP1) , were evaluated with western-blot to explore Tan IIA effect on mTOR pathway. From the Fig.6B, Tan IIA indeed inhibited the phosphorylated activation of Akt and mTOR stimulated by

20 ng/mL TNF-α. Meanwhile, the increased phosphorylation of p70S6K and 4E-BP1 triggered by TNF-α is also inhibited by Tan IIA treatment in concentration-dependent manner, suggesting Tan IIA suppressed Akt/mTOR/ p70S6K and 4E-BP1 signaling pathway in RA-FLSs.

Additionally, from the results of GO and KEGG analysis the HIF-1 pathway is a potential target for Tan IIA. The molecular mechanism of hypoxia sensitivity involves oxygen sensing hydroxylases, prolyl-hydroxylases, orchestrating two main transcription factors related to induction of inflammation and angiogenesis, namely nuclear factor-κB (NFκB) and HIF-1(D'Ignazio and Rocha, 2016; Fearon and Canavan et al., 2016). Therefore, we detected the effect of Tan IIA on the HIF-1α and NFκB expression variation in RA-FLSs. Similarly, Tan IIA also suppressed the phosphorylated level of NFκB p65 and upstream Iκκα (Fig. 5C) and the HIF-1α expression (Fig. 5D) stimulated with TNF-α, which indicated Tan IIA could participate in regulating the response of synovial tissues to hypoxia. Altogether, the regulation of the RA-FLSs biological characteristics by Tan IIA is dependent on dissuading not only intracellular phosphorylated activation of MAPK and Akt/mTOR pathway but expression and activation of HIF-1α and NFκB.

## DISCUSSION

RA is a chronic autoimmune disease with a hyperplastic, aggressive and invasive phenotype that causes the formation of pannus angiogenesis, inflammation, cartilage degradation, and subsequent bone erosion (Smolen and Aletaha et al., 2016). RA-FLSs take key lead in the pathogenesis of inflammatory arthritis due to their tumor-like features of proliferation, migration and invasion (Karami and Aslani et al., 2019). In this context, RA-FLSs stand out as a potential target for RA treatment (de Oliveira and Farinon et al., 2019). Currently, the main RA treatment strategies in clinical practice are chemical drugs, including non-steroidal anti-inflammatory drugs (NSAIDs), disease-modifying anti-rheumatic drugs (DMARDs) and

glucocorticoids(Conigliaro and Triggianese et al., 2019). Nevertheless, these treatments are usually associated with adverse reactions, such as cardiovascular and gastrointestinal bleeding risk, liver and kidney toxicity, growth inhibition, infection and tumor risk (Yamamoto and Mimori et al., 2011; Rubbert-Roth and Petereit, 2012; Xue and Cohen et al., 2016; Nissen, 2017; Wang and Zhou et al., 2018). In recent years, the progress of research on the pathogenesis of RA has resulted in the development of new anti-rheumatic drugs, such as biological agents and small molecule targeted signaling pathway inhibitors. These new drugs have greatly improved the chronic inflammatory state and quality of life of RA patients (Conigliaro and Triggianese et al., 2019). However, clinical data show that only less than 50% of RA patients can benefit from these new drugs. Unfortunately, more than 30% of patients still suffer from unsatisfactory disease control and more than 20% of RA patients are unable to effectively control disease activities. In such cases, the bone destruction process cannot be blocked or delayed, even after the clinical use of these recent drugs (Ranganath and Motamedi et al., 2015; Smolen and Aletaha et al., 2016; Conigliaro and Triggianese et al., 2019).

Recently, herbal medicines have received great scientific attention for their remarkable healing effects and for having fewer side effects than synthetic drugs. The therapeutic effects of Tan IIA, a compound isolated from *Salviae miltiorrhizae*, includes pro-apoptotic, anti-tumor and anti-inflammatory activities. Additionally, Tang, et al. showed that Tan IIA injections could inhibit the inflammatory response in PBMCs of RA patients by decreasing TNF-$\alpha$ and IL-6 levels (Tang and Zhou et al., 2019). Therefore, the application of Tan IIA in the treatment of RA is feasible in terms of therapeutic effect. To highlight the potential of Tan IIA for RA treatment, we first used AIA mice model to verify its therapeutic effects. The AIA model has been widely used in clarifying the pathogenesis of RA and to explore potential therapeutic targets, including the validation of the therapeutic effects of new drugs (Sardar and Andersson, 2016; Atkinson and Nansen, 2017; Dong and Wu et al., 2019; Du and Zhang et al.,

2019). Our experiments showed that AIA mice treat with Tan IIA showed decreased histologic scores and alleviated synovial inflammation. The level of the inflammatory cytokines, including IL-6, IL-17 and TNF-α, measured after 40 days of treatment was significantly higher in the AIA model group than in normal group. However, the level of inflammatory cytokines was significantly lower in AIA mice treated with Tan IIA than in the AIA model group. The data obtained using AIA model showed that Tan IIA not only reduced the swelling of knee joint caused by inflammation, but also inhibited the expression of pro-inflammatory factors and improved the pathological manifestations of AIA mice. These data corroborate our initial hypothesis that Tan IIA has therapeutic potential for RA treatment. To date, few in vivo studies on Tan IIA effects for RA treatment have been conducted and no detailed related mechanisms had been discovered.

To discover the mechanisms involved in the effects of Tan IIA on RA, we constructed primary RA-FLS strains from samples of synovial tissue from RA patients. We demonstrated that Tan IIA can inhibit the tumor-like proliferation characteristics of RA-FLSs in clinically safe concentrations. According to our data, although Tan IIA does not have a remarkable effect on the vitality of RA-FLSs after 24h treatment, it can prevent TNF-α-stimulated cell proliferation in a dose-dependent manner after 48h of treatment. In addition, previous reports suggested that high concentrations Tan IIA can promote RA-FLSs apoptosis (Jie and Du H et al., 2014; Li and Liu et al., 2018) and probably by up-regulating lncRNA GAS5 (Li and Liu et al., 2018). However, we found in our experiments that RA-FLSs do not undergo apoptosis when treated with up to 20μM of Tan IIA, while cell apoptosis maybe accrue at the concentration of Tan IIA over 40μM. Therefore, we speculate that the effect of Tan IIA on RA-FLSs is different between higher and lower concentrations of Tan IIA, although further studies are needed to elucidate this issue. Moreover, Tan IIA could restrict the migration and invasion of RA-FLSs, which would be better for suppressing the tumor-like properties of RA-FLSs and reducing the damage to distal cartilages.

The RA pathogenesis states that RA-FLSs usually secrete pro-inflammatory factors and chemokines, including TNF-α, IL-6, IL-8, IL-17 and IL-1β, to recruit and activate various immune cells. These immune cells, in turn, secrete cytokines to activate RA-FLSs, contributing to cartilage damage and joint destruction (Bartok and Firestein, 2010; Bottini and Firestein, 2013). TNF-α is one of the most important inflammatory cytokines in the joint cavity of RA patients and is commonly used as an activator of RA-FLSs in vitro to simulate the inflammatory microenvironment (Shi and Wang et al., 2018; Du and Zhang et al., 2019; Wang and Li et al., 2019; Wu and Li et al., 2019). We found that 20ng/mL of exogenous TNF-α can stimulate RA-FLSs and produce a similar effect. It is worth mentioning that 10 or 20μM of Tan IIA inhibited the increased mRNA expression of IL-6, IL-1β and IL-8 induced by 20ng/mL of TNF-α. Moreover, only 1μM of sodium tanshinone IIA sulfonate, a Tan IIA derivate, can decrease IL-6 and IL-1β mRNA expression (Wang and Li et al., 2019). Taken together, these data suggest that Tan IIA acts as an anti-inflammatory in RA by inhibiting the production of pro-inflammatory cytokines, despite the different worked concentrations of Tan IIA or its derivative. Remarkably, Tan IIA did not inhibit TNF-α-induced IL-17 mRNA expression, which wes similar with our previous reserach on 3′3-Diindolylmethane (DIM) (Du and Zhang et al., 2019). This may related to the individual differences of the patients or that IL-17 production is not related to TNF-α stimulation, and, therefore, it is regulated by other mechanisms. From ELISA results, we observed that, although there was no increase in TNF-α-induced IL-8, 20μM of Tan IIA suppressed the release of IL-8 by RA-FLSs. Moreover, we also found that Tan IIA inhibited the tendency of IL-1β increase induced by TNF-α, although the basal expression of IL-1β in the blank control group was difficult to detect because it was low.

Previous studies suggested that the expression of MMPs in fibroblasts of synovial joints is responsible for the degradation of synovial collagen in several inflammatory diseases, including RA (Agere and Akhtar et al., 2017) . More than fifteen synovial MMPs are expressed in the synovial joints from RA patients and they fall into three

554 main categories: collagenase, gelatinase, and matrix metalloproteinase (Konttinen and
555 Ainola et al., 1999). We found that 20μM of Tan IIA prevented TNF-α-induced mRNA
556 expression of MMP-8 collagenase, MMP-2 and MMP-9 gelatinases and MMP-3 matrix
557 metalloproteinase. However, we were unable to detect these MMPs at protein level in
558 the culture supernatant, similar to previous studies (Du and Zhang et al., 2019). Despite
559 the absence of bands in western-blot and Gelatinase analyzes, our data suggest that
560 these MMPs did indeed play an important role in the invasion and migration of RA-
561 FLSs. In addition, we demonstrated that Tan IIA decreased the expression of MMPs in
562 RA-FLSs.

563 Tan IIA has been reported to affect the proliferation, invasion and migration of
564 tumor cells through different signaling pathways (Zhang and Guo et al., 2018; Liao and
565 Gao et al., 2019; Xue and Jin et al., 2019). However, the specific molecular mechanism
566 of Tan IIA in RA-FLSs is still unknown. We performed network pharmacology
567 analyzes and found some potential pathways for Tan IIA action in the treatment of RA.
568 The integration of the network pharmacology analyzes with the experimental in vitro
569 obtained data reveals that Tan IIA can affect three different pathways, which are:
570 MAPK, AKT/mTOR, HIF-1 and NF-kB.

571 Mitogen-activated protein kinases (MAPK) family is widely conserved among
572 eukaryotes and is responsible for the phosphorylation and dephosphorylation of
573 several key proteins involved in regulatory mechanisms of different cells (Tong and
574 Wan et al., 2014). Extracellular signal regulated kinase (ERK), c-Jun N-terminal
575 kinase (JNK) and P38MAP kinase (p38) are the main members of the MAPK family.
576 These proteins are the main intracellular responders embedded in a highly active
577 signaling flow that is involded in the activation of RA-FLSs (Muller-Ladner and
578 Ospelt et al., 2007; Tong and Wan et al., 2014; Bustamante and Garcia-Carbonell et
579 al., 2017). Several compounds, including sodium tanshinone IIA sulfonate, DIM and
580 triptolide, have been shown to inhibit MAPK signaling pathway activation by
581 preventing the phosphorylation of p38, JNK, and ERK. Thus, these compounds are

able to inhibit the proliferation, metastasis and invasion of RA-FLSs (Yang and Ye et al., 2016; Du and Zhang et al., 2019; Wang and Li et al., 2019). Our data showed that Tan IIA played an inhibitory role in TNF-α-stimulated p38 and JNK phosphorylation in RA-FLSs, but had no significant effect on ERK. Therefore, we suggest that the effect of Tan IIA on proliferation, migration and invasion in RA-FLSs is mainly mediated by inactivation of p38 and JNK proteins. There is practically a consensus that the expression and activation of p38 and JNK in the synovial tissue of RA patients modulate the growth, apoptosis and differentiation of RA-FLSs. Thus, inflammation and cartilage damage is triggered in the joint cavity of RA patients (Yang and Ye et al., 2016; Bustamante and Garcia-Carbonell et al., 2017).

The PI3K/AKT signaling pathway is involved in the pathogenesis of inflammation (Malemud, 2015) and, therefore, understand its regulation would be a great benefit for the control of RA (Laragione and Gulko, 2010; Jia and Cheng et al., 2015). mTOR complex 1 (mTORC1) lies downstream of the PI3K/Akt pathway. The activation of the downstream signaling through AKT-mediated mTORC1 phosphorylation promotes anabolic processes and limits catabolic processes involved in cell growth, proliferation and metabolism (Liu and Li et al., 2006; Laplante and Sabatini, 2009). Moreover, previous reports have shown that activation of PI3K/AKT/mTOR pathway appears to be the critical driver of proliferation and anti-apoptosis responses, that is a typically feature of inflamed synovial tissue of RA (Garcia and Liz et al., 2010). Cytokines, especially TNF-α in RA-FLS lead to activation of the PI3K/AKT/mTOR pathway, thereby promoting cell migration and invasion (Karonitsch and Kandasamy et al., 2018). Moreover, S6K1 and 4E-BP1 are the two best characterized mTORC1 substrates, whereby mTORC1 plays the role of a mRNA to protein translator (Wendel and De Stanchina et al., 2004). In our data, we found direct evidences that Tan IIA can influence the AKT/mTOR pathway. We showed that Tan IIA blocks activation by TNF-α-stimulated phosphorylation of AKT/mTOR and downstream p70S6K and 4E-BP1. Therefore, these data indicate that Tan IIA has

antiproliferative activity and highlight that Tan IIA can be used independently or in combination with other drugs to improve clinical symptoms in RA patients. On the other hand, numerous studies have revealed that autophagy and autophagy-related proteins also participate in the pathogenesis and progress of RA. Furthermore, the mTOR pathway is also involved with autophagy in RA (Li and Chen et al., 2017; Wu and Adamopoulos, 2017). Further studies are needed to assess whether Tan IIA can regulate RA-FLSs autophagy via AKT/mTOR pathway.

Insufficient oxygen supply appears in the damaged articular cavity in RA pathology and is accompanied by metabolic disorders and pannus hyperplasia, resulting in a hypoxic microenvironment (Fearon and Canavan et al., 2016; Quinonez-Flores and Gonzalez-Chavez et al., 2016; Veale and Orr et al., 2017). The transcription factors NF-κB and HIFs, in addition to the relative enzymes, oxygen-sensitive and prolyl hydroxylases, are responsible for responding to the hypoxia signal in the hypoxic microenvironment. In particular, NF-κB and HIFs play key roles in several disorders, including induction of inflammation and angiogenesis and rheumatoid arthritis (Szade and Grochot-Przeczek et al., 2015; D'Ignazio and Rocha, 2016). Our analysis showed that HIF-1 pathway may be a potential target for Tan IIA in RA. Based on previous data, we chose NF-κB p65 and HIF-1α as targets to assess their changes in response to hypoxia to highlight the effect of Tan IIA on hypoxia pathways. Our data showed that Tan IIA can actually inhibit HIF-1α expression and TNF-α-stimulated NFκB p65 phosphorylation. Moreover, Tan IIA can also decrease LPS-induced p65 protein expression in PBMCs of RA patients (Tang and Zhou et al., 2019). Therefore, it can be concluded that Tan IIA may affects RA by suppressing HIF-1α and NF-κB p65 to alleviate the damage of hypoxia and the release of proinflammatory cytokines. Nevertheless, the regulatory mechanism of HIF-1α and NF-κB p65 needs further studies to be fully revealed.

In conclusion, our data reveal a specific role of Tan IIA on TNF-dependent arthritogenesis. We identified that Tan IIA can inhibit the proliferation, migration and

invasion of RA-FLSs and suppress the release of proinflammatory cytokines and MMPs. We have also shown that Tan IIA achieves these effects by affecting MAPK, AKT/mTOR, HIF-1 and NF-κB signaling pathways. Finally, we present in vivo evidence that Tan IIA is able to improve the arthritis severity in AIA mice. .Therefore, this study highlights the therapeutic role of Tan IIA in the treatment of RA and shows its potential to improve the quality life of RA patients.

## DATA AVAILABILITY

All datasets generated for this study are included in the manuscript and the Supplementary Files.

## ETHICS STATEMENT

Our study was authorized by the Medical Ethics Committee of the Zhujiang Hospital, Southern Medical University. All patients voluntarily signed informed consent. All the animal experiments were conducted with approval of the Southern Medical University Ethics Committee for Animal Laboratory Research. Animal care and handling procedures abided by the guidelines of ethical regulations for institutional animal care used in the Southern Medical University.

## AUTHOR CONTRIBUTIONS

Design the entire study: HD, YW, and LJ. Experimental studies: HD, YZ, XH, DL, LY and JW. Network pharmacology analysis: YW. Animal model construction: YL and XC. the experimental data analysis and statistic: HD, HL and LJ. Write and revise the manuscript: HD, HY, YW and LJ. All authors read and approved the final manuscript.

## CONFLICT OF INTEREST STATEMENT

The authors declare that the research achieved without any commercial or financial relationships and there are no competing interests associated with the manuscript.

**ACKNOWLEGEMENTS**

This work was supported by grants from the National Natural Science Foundation of China (81601397，81771727, 81102688 and 81401920), Natural Science Foundation of Guangdong Province (2016A030313624), Program from Guangdong Innovation and Entrepreneurship training for college students (201812121108) and Scientific Enlightenment Project from Southern Medical University. Additionally, we thank Ningchao Du, Wei Wang, Quanbao Wu, Yuefan Chen, Qiong Li and Yuting Chen for some technical assistance during the experiments.

# References:

Agere, S. A. and N. Akhtar, et al. (2017). "RANTES/CCL5 Induces Collagen Degradation by Activating MMP-1 and MMP-13 Expression in Human Rheumatoid Arthritis Synovial Fibroblasts." Front Immunol **8**: 1341.

Arnett, F. C. and S. M. Edworthy, et al. (1988). "The American Rheumatism Association 1987 revised criteria for the classification of rheumatoid arthritis." Arthritis Rheum **31** (3): 315-24.

Atkinson, S. M. and A. Nansen (2017). "Pharmacological Value of Murine Delayed-type Hypersensitivity Arthritis: A Robust Mouse Model of Rheumatoid Arthritis in C57BL/6 Mice." Basic Clin Pharmacol Toxicol **120** (2): 108-114.

Baradaran-Heravi, A. and A. D. Balgi, et al. (2016). "Novel small molecules potentiate premature termination codon readthrough by aminoglycosides." Nucleic Acids Res **44** (14): 6583-98.

Bartok, B. and G. S. Firestein (2010). "Fibroblast-like synoviocytes: key effector cells in rheumatoid arthritis." Immunol Rev **233** (1): 233-55.

Bottini, N. and G. S. Firestein (2013). "Duality of fibroblast-like synoviocytes in RA: passive responders and imprinted aggressors." Nat Rev Rheumatol **9** (1): 24-33.

688 Bustamante, M. F. and R. Garcia-Carbonell, et al. (2017). "Fibroblast-like synoviocyte metabolism in
689 the pathogenesis of rheumatoid arthritis." Arthritis Res Ther **19** (1): 110.

690 Chen, Z. and H. Xu (2014). "Anti-Inflammatory and Immunomodulatory Mechanism of Tanshinone IIA
691 for Atherosclerosis." Evid Based Complement Alternat Med **2014**: 267976.

692 Conigliaro, P. and P. Triggianese, et al. (2019). "Challenges in the treatment of Rheumatoid Arthritis."
693 Autoimmun Rev **18** (7): 706-713.

694 de Oliveira, P. G. and M. Farinon, et al. (2019). "Fibroblast-Like Synoviocytes Glucose Metabolism as
695 a Therapeutic Target in Rheumatoid Arthritis." Front Immunol **10**: 1743.

696 D'Ignazio, L. and S. Rocha (2016). "Hypoxia Induced NF-kappaB." Cells **5** (1).

697 Dong, L. and J. Wu, et al. (2019). "Mannan-Binding Lectin Attenuates Inflammatory Arthritis Through
698 the Suppression of Osteoclastogenesis." Front Immunol **10**: 1239.

699 Du, H. and X. Zhang, et al. (2019). "A Novel Phytochemical, DIM, Inhibits Proliferation, Migration,
700 Invasion and TNF- α Induced Inflammatory Cytokine Production of Synovial Fibroblasts From
701 Rheumatoid Arthritis Patients by Targeting MAPK and AKT/mTOR Signal Pathway." Frontiers in
702 Immunology **10**: 1620.

703 Fearon, U. and M. Canavan, et al. (2016). "Hypoxia, mitochondrial dysfunction and synovial
704 invasiveness in rheumatoid arthritis." Nat Rev Rheumatol **12** (7): 385-97.

705 Frey, O. and M. Huckel, et al. (2018). "Induction of chronic destructive arthritis in SCID mice by
706 arthritogenic fibroblast-like synoviocytes derived from mice with antigen-induced arthritis." Arthritis
707 Res Ther **20** (1): 261.

708 Garcia, S. and M. Liz, et al. (2010). "Akt activity protects rheumatoid synovial fibroblasts from Fas-
709 induced apoptosis by inhibition of Bid cleavage." Arthritis Res Ther **12** (1): R33.

710 Gou, K. J. and R. Zeng, et al. (2018). "Anti-rheumatoid arthritis effects in adjuvant-induced arthritis in
711 rats and molecular docking studies of Polygonum orientale L. extracts." Immunol Lett **201**: 59-69.

712 Grotsch, B. and A. Bozec, et al. (2019). "In Vivo Models of Rheumatoid Arthritis." Methods Mol Biol
713 **1914**: 269-280.

714 Hu, F. and H. R. Hepburn, et al. (2005). "Effects of ethanol and water extracts of propolis (bee glue) on
715 acute inflammatory animal models." J Ethnopharmacol **100** (3): 276-83.

716 Huber, L. C. and O. Distler, et al. (2006). "Synovial fibroblasts: key players in rheumatoid arthritis."
717 Rheumatology (Oxford) **45** (6): 669-75.

718 Jia, P. T. and X. L. Zhang, et al. (2017). "Articular cartilage degradation is prevented by tanshinone IIA
719 through inhibiting apoptosis and the expression of inflammatory cytokines." Mol Med Rep **16** (5): 6285-
720 6289.

721 Jia, Q. and W. Cheng, et al. (2015). "Cucurbitacin E inhibits TNF-alpha-induced inflammatory cytokine
722 production in human synoviocyte MH7A cells via suppression of PI3K/Akt/NF-kappaB pathways." Int
723 Immunopharmacol **29** (2): 884-890.

724 Jie, L. G. and R. Y. Huang, et al. (2015). "Role of cysteinerich angiogenic inducer 61 in fibroblastlike
725 synovial cell proliferation and invasion in rheumatoid arthritis." Mol Med Rep **11** (2): 917-23.

726 Jie, L. and Du H, et al. (2014). "Tanshinone IIA induces apoptosis in fibroblast-like synoviocytes in
727 rheumatoid arthritis via blockade of the cell cycle in the G2/M phase and a mitochondrial pathway." Biol
728 Pharm Bull **37** (8): 1366-72.

729 Jie, L. and Q. Huang, et al. (2002). "The curative effect evaluation of salvia miltiorrhiza on RA." Chinese
730 Journal of Clinical Rebabilitation **6** (14): 2301.

731 Jie, L. and Q. Huang, et al. (2010). "Clinical observation of compound salvia injection in patients with
732 active RA." Liaoning journal of traditional Chinese medicine **37** (10): 1945-1948.

733 Karami, J. and S. Aslani, et al. (2019). "Epigenetics in rheumatoid arthritis; fibroblast-like synoviocytes
734 as an emerging paradigm in the disease pathogenesis." Immunol Cell Biol.

735 Karonitsch, T. and R. K. Kandasamy, et al. (2018). "mTOR Senses Environmental Cues to Shape the
736 Fibroblast-like Synoviocyte Response to Inflammation." Cell Rep **23** (7): 2157-2167.

737 Konttinen, Y. T. and M. Ainola, et al. (1999). "Analysis of 16 different matrix metalloproteinases (MMP-
738 1 to MMP-20) in the synovial membrane: different profiles in trauma and rheumatoid arthritis." Ann
739 Rheum Dis **58** (11): 691-7.

740 Laplante, M. and D. M. Sabatini (2009). "mTOR signaling at a glance." J Cell Sci **122** (Pt 20): 3589-94.

741 Laragione, T. and P. S. Gulko (2010). "mTOR regulates the invasive properties of synovial fibroblasts
742 in rheumatoid arthritis." Mol Med **16** (9-10): 352-8.

743 Lefevre, S. and A. Knedla, et al. (2009). "Synovial fibroblasts spread rheumatoid arthritis to unaffected
744 joints." Nat Med **15** (12): 1414-20.

745 Li, G. and Y. Liu, et al. (2018). "Tanshinone IIA promotes the apoptosis of fibroblast-like synoviocytes
746 in rheumatoid arthritis by up-regulating lncRNA GAS5." Biosci Rep **38** (5).

747 Li, S. and J. W. Chen, et al. (2017). "Autophagy inhibitor regulates apoptosis and proliferation of

synovial fibroblasts through the inhibition of PI3K/AKT pathway in collagen-induced arthritis rat model." Am J Transl Res **9** (5): 2065-2076.

Liao, X. Z. and Y. Gao, et al. (2019). "Tanshinone IIA combined with cisplatin synergistically inhibits non-small-cell lung cancer in vitro and in vivo via down-regulating the phosphatidylinositol 3-kinase/Akt signalling pathway." Phytother Res **33** (9): 2298-2309.

Liu, L. and F. Li, et al. (2006). "Rapamycin inhibits cell motility by suppression of mTOR-mediated S6K1 and 4E-BP1 pathways." Oncogene **25** (53): 7029-40.

Liu, Z. and W. Zhu, et al. (2019). "Tanshinone IIA inhibits glucose metabolism leading to apoptosis in cervical cancer." Oncol Rep **42** (5): 1893-1903.

Malemud, C. J. (2015). "The PI3K/Akt/PTEN/mTOR pathway: a fruitful target for inducing cell death in rheumatoid arthritis?" Future Med Chem **7** (9): 1137-47.

Muller-Ladner, U. and C. Ospelt, et al. (2007). "Cells of the synovium in rheumatoid arthritis. Synovial fibroblasts." Arthritis Res Ther **9** (6): 223.

Nissen, S. E. (2017). "Cardiovascular Safety of Celecoxib, Naproxen, or Ibuprofen for Arthritis." N Engl J Med **376** (14): 1390.

Quinonez-Flores, C. M. and S. A. Gonzalez-Chavez, et al. (2016). "Hypoxia and its implications in rheumatoid arthritis." J Biomed Sci **23** (1): 62.

Ranganath, V. K. and K. Motamedi, et al. (2015). "Comprehensive appraisal of magnetic resonance imaging findings in sustained rheumatoid arthritis remission: a substudy." Arthritis Care Res (Hoboken) **67** (7): 929-39.

Ren, J. and L. Fu, et al. (2019). "Salvia miltiorrhiza in Treating Cardiovascular Diseases: A Review on Its Pharmacological and Clinical Applications." Front Pharmacol **10**: 753.

Rubbert-Roth, A. and H. F. Petereit (2012). "[Nervous system side effects of disease modifying treatments of rheumatoid arthritis]." Z Rheumatol **71** (7): 572-82.

Sardar, S. and A. Andersson (2016). "Old and new therapeutics for Rheumatoid Arthritis: in vivo models and drug development." Immunopharmacol Immunotoxicol **38** (1): 2-13.

Shi, M. and J. Wang, et al. (2018). "Glycogen Metabolism and Rheumatoid Arthritis: The Role of Glycogen Synthase 1 in Regulation of Synovial Inflammation via Blocking AMP-Activated Protein Kinase Activation." Front Immunol **9**: 1714.

Smolen, J. S. and D. Aletaha, et al. (2016). "Rheumatoid arthritis." Lancet **388** (10055): 2023-2038.

778 Sui, H. and J. Zhao, et al. (2017). "Tanshinone IIA inhibits beta-catenin/VEGF-mediated angiogenesis
779 by targeting TGF-beta1 in normoxic and HIF-1alpha in hypoxic microenvironments in human colorectal
780 cancer." Cancer Lett **403**: 86-97.

781 Szade, A. and A. Grochot-Przeczek, et al. (2015). "Cellular and molecular mechanisms of inflammation-
782 induced angiogenesis." IUBMB Life **67** (3): 145-59.

783 Tang, J. and S. Zhou, et al. (2019). "Inhibitory effect of tanshinone IIA on inflammatory response in
784 rheumatoid arthritis through regulating beta-arrestin 2." Exp Ther Med **17** (5): 3299-3306.

785 Ting, Z. and L. Hongyan, et al. (2017). "WITHDRAWN: Anti-arthritic effect of pilose antler peptide on
786 adjuvant-induced rheumatoid arthritis in rats." Int J Biol Macromol.

787 Tong, B. and B. Wan, et al. (2014). "Role of cathepsin B in regulating migration and invasion of
788 fibroblast-like synoviocytes into inflamed tissue from patients with rheumatoid arthritis." Clin Exp
789 Immunol **177** (3): 586-97.

790 Veale, D. J. and C. Orr, et al. (2017). "Cellular and molecular perspectives in rheumatoid arthritis." Semin
791 Immunopathol **39** (4): 343-354.

792 Wang, J. and Q. Zhao (2019). "Kaempferitrin inhibits proliferation, induces apoptosis, and ameliorates
793 inflammation in human rheumatoid arthritis fibroblast-like synoviocytes." Phytother Res **33** (6): 1726-
794 1735.

795 Wang, R. and Z. Luo, et al. (2019). "Tanshinone IIA Reverses Gefitinib-Resistance In Human Non-
796 Small-Cell Lung Cancer Via Regulation Of VEGFR/Akt Pathway." Onco Targets Ther **12**: 9355-9365.

797 Wang, W. and H. Zhou, et al. (2018). "Side effects of methotrexate therapy for rheumatoid arthritis: A
798 systematic review." Eur J Med Chem **158**: 502-516.

799 Wang, Z. and J. Li, et al. (2019). "Sodium tanshinone IIA sulfonate inhibits proliferation, migration,
800 invasion and inflammation in rheumatoid arthritis fibroblast-like synoviocytes." Int Immunopharmacol
801 **73**: 370-378.

802 Wendel, H. G. and E. De Stanchina, et al. (2004). "Survival signalling by Akt and eIF4E in oncogenesis
803 and cancer therapy." Nature **428** (6980): 332-7.

804 Wu, D. J. and I. E. Adamopoulos (2017). "Autophagy and autoimmunity." Clin Immunol **176**: 55-62.

805 Wu, J. and Q. Li, et al. (2019). "Kirenol Inhibits the Function and Inflammation of Fibroblast-like
806 Synoviocytes in Rheumatoid Arthritis in vitro and in vivo." Front Immunol **10**: 1304.

807 Xue, J. and X. Jin, et al. (2019). "Effects and Mechanism of Tanshinone II A in Proliferation, Apoptosis,

and Migration of Human Colon Cancer Cells." Med Sci Monit **25**: 4793-4800.

Xue, Y. and J. M. Cohen, et al. (2016). "Skin Signs of Rheumatoid Arthritis and its Therapy-Induced Cutaneous Side Effects." Am J Clin Dermatol **17** (2): 147-62.

Yamamoto, K. and T. Mimori, et al. (2011). "[Discussion meeting on treatment of rheumatoid arthritis with biologics and their side effects]." Nihon Naika Gakkai Zasshi **100** (10): 2998-3017.

Yang, Y. and Y. Ye, et al. (2016). "Triptolide inhibits the migration and invasion of rheumatoid fibroblast-like synoviocytes by blocking the activation of the JNK MAPK pathway." Int Immunopharmacol **41**: 8-16.

Zhang, L. and W. Lin, et al. (2019). "Tanshinone IIA reverses EGF- and TGF-beta1-mediated epithelial-mesenchymal transition in HepG2 cells via the PI3K/Akt/ERK signaling pathway." Oncol Lett **18** (6): 6554-6562.

Zhang, S. and G. Huang, et al. (2017). "Tanshinone IIA ameliorates chronic arthritis in mice by modulating neutrophil activities." Clin Exp Immunol **190** (1): 29-39.

Zhang, Y. and S. Guo, et al. (2018). "Tanshinone IIA inhibits cell proliferation and tumor growth by downregulating STAT3 in human gastric cancer." Exp Ther Med **16** (4): 2931-2937.

# LEGENDS

**FIGURE 1|** Study design of the AIA experiment. Male C57BL/6 mice aged 10-12weeks were immunized at each sides of knee articular cavity on day 0, and second immunizations were operated on day 21. From day 2 to day 31 after immunizing, mice were administered with oral gavage Tan IIA once a day consecutively as described in the Materials and Methods. Body weight and knee joint diameter were measured every 5 days. The blood samples were collected for proinflammatory cytokines analysis on day 40, 48, 56 and 80. The mice were euthanized at day 80, and bone, spleen, liver and serum samples were collected. The bones of knee joints were applied to Histopathological analysis. Spleen and liver indices were calculated by weighing spleen and liver. The serum samples were applied to the ELISA assay.

**FIGURE 2** | Tan IIA ameliorates arthritis severity in mice with AIA. **(A)** The effect of Tan IIA on mean change in body weight of mice after immunization (from day 0 to day 80) monitored every 5 days. **(B)** The effect of Tan IIA on mean change in knee joint diameter after immunization (from day 0 to day 80) monitored every 5 days. **(C)** The effect of Tan IIA on the spleen and liver index of mice with AIA and control. Data shown as spleen weight (g)/body weight (g) ×100%. **(D)** The effect of Tan IIA on the pathohistological features of knee joints in mice with AIA. Photomicrographs for knee joint sections stained with H&E (original magnification 200 ×). **(E)** The scores for inflammatory severity. **(F)**The effect of Tan IIA on IL-6, IL-17 and TNF-α expression in serum of mice with AIA and control after immunization on day 40, 48, 56 and 80. All the data were expressed as means ± S.D. n=6, $^{*}P < 0.05$, $^{**}P < 0.01$, $^{***}P < 0.001$ vs. the control group, $^{\#}P < 0.05$, $^{\#\#}P < 0.01$, $^{\#\#\#}P < 0.001$ vs. AIA model group.

**FIGURE 3** | Tan IIA Suppresses the migration and invasion of RA-FLSs. **(A)** The effect of Tan IIA on migration was detected with transwell Boyden chamber after 8 and 12h. The images are representative of migration or invasion through the membrane after staining. Original magnification 200× (left panel). Cell numbers/field were presented as the mean ± SD of eight independent fields (right panel). **(B)** The effect of Tan IIA on invasion was detected with transwell Boyden chamber coated with a Matrigel basement membrane matrix after 12 and 24h. The images are representative of migration or invasion through the membrane after staining. Original magnification 200× (left panel). Cell numbers/field were presented as the mean ± SD of eight independent fields (right panel). **(C)** The effect of Tan IIA on wound healing was detected with cell scratching assay. After 48h the wound area was photographed

using microscope. Original magnification 100× (left panel). The extent of wound closure was presented as the percentage by which the original scratch width had decreased at each measured time point. The values are the mean ± SEM from at least 3 independent experiments (right panel). $^{*}P < 0.05$, $^{**}P < 0.01$, $^{***}P < 0.001$ vs. 0 μM (Ctrl).

**FIGURE 4** | The effect of Tan IIA on producing pro-inflammatory cytokines and MMPs of RA-FLSs. **(A)** the effect of 0, 2.5, 5, 10 and 20μM Tan IIA on cell viability induced by TNF-α(20ng/mL). **(B)** The effect of 10μM and 20μM Tan IIA on relative mRNA expression of pro-inflammatory cytokines induced by TNF-α (20ng/mL) to β-actin in RA-FLSs. **(C)** The effect of 10μM and 20μM Tan IIA on relative mRNA expression of MMP-2, MMP-3, MMP-8 and MMP-9 induced by TNF-α (20ng/mL) to β-actin in RA-FLSs. **(D)** The effect of Tan IIA on pro-inflammatory cytokines releasing induced by TNF-α in RA-FLSs. a. the effect of 10μM and 20μM Tan IIA on IL-6 releasing induced by TNF-α (20ng/mL). b. the effect of 10μM and 20μM Tan IIA on IL-1β releasing induced by TNF-α (20ng/mL). c. the effect of 10μM and 20μM Tan IIA on IL-8 releasing induced by TNF-α (20ng/mL). The values are the mean ± SEM from at least 3 independent experiments. $^{*}P < 0.05$, $^{**}P < 0.01$, $^{***}P < 0.001$vs. Ctrl (0 μM Tan IIA and 0ng/mL TNF-α). $^{\#}P < 0.05$, $^{\#\#}P < 0.01$, $^{\#\#\#}P < 0.001$ vs. group treated by TNF-α (20ng/mL).

**FIGURE 5**| Enrichment analysis of Tan Ⅱ A against rheumatoid arthritis: **(A)** Venn diagram revealing the overlapping target genes of Tan Ⅱ A against rheumatoid arthritis. **(B)** Protein interaction network of the overlapping target genes of Tan Ⅱ A against rheumatoid arthritis. Each network node represents all the proteins produced by a single, protein-coding gene locus, and the edge represents protein-protein associations. **(C)** KEGG enrichment and network analysis of RA target genes. Top 20 functionally enriched biological processes with corresponding adjusted *p*-values analyzed, which are displayed in a dot plot. The color scales indicated the different thresholds of adjusted p-values, and the sizes of the dots represented the gene count of each term.

**FIGURE 6**| The effect of Tan IIA on the intracellular phosphorylated activation of MAPK and Akt/mTOR pathway induced by TNF-α in RA-FLSs. RA-FLSs were treated with TNF-α(20ng/mL) or/and Tan IIA (10 and 20μM) for 24 h, **(A)** Western blot analysis was conducted to assess the expression and phosphorylation level of p38MAPK, JNK, ERK and FAK. Representative images of immune blot (left panel) and densitometric quantification phosphorylation/total of p38MAPK, JNK and ERK expression (right panel). **(B)** Western blot analysis was conducted to assess the expression and phosphorylation level of AKT, mTOR, p70S6K and 4E-BP1.

Representative images of immune blot (left panel) and densitometric quantification phosphorylation/total of AKT, mTOR, p70S6K and 4E-BP1 expression (right panel). **(C)** Western blot analysis was conducted to assess the expression and phosphorylation level of Ικκα and NFκB p65. Representative images of immune blot (left panel) and densitometric quantification phosphorylation/total of Ικκα and NFκB p65 expression (right panel). **(D)** Western blot analysis was conducted to assess the expression level of HIF-α. Representative images of immune blot (left panel) and densitometric quantification of HIF-α expression (right panel). Densitometry analysis from three independent experiments was used to quantitate the protein expression. $^{*}P < 0.05$, $^{**}P < 0.01$, $^{***}P < 0.001$vs. Ctrl (0 μM Tan IIA), $^{\#}P < 0.05$, $^{\#\#}P < 0.01$, $^{\#\#\#}P < 0.001$ vs. group treated by TNF-α (20ng/mL).

913 **Fig.1**

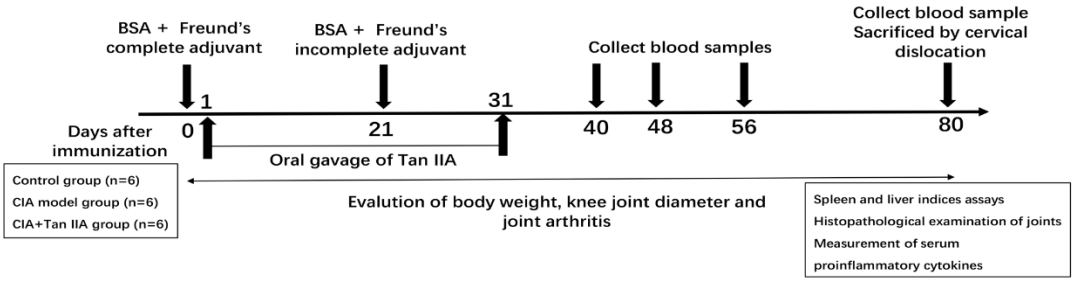


914

915

916 **Fig.2**

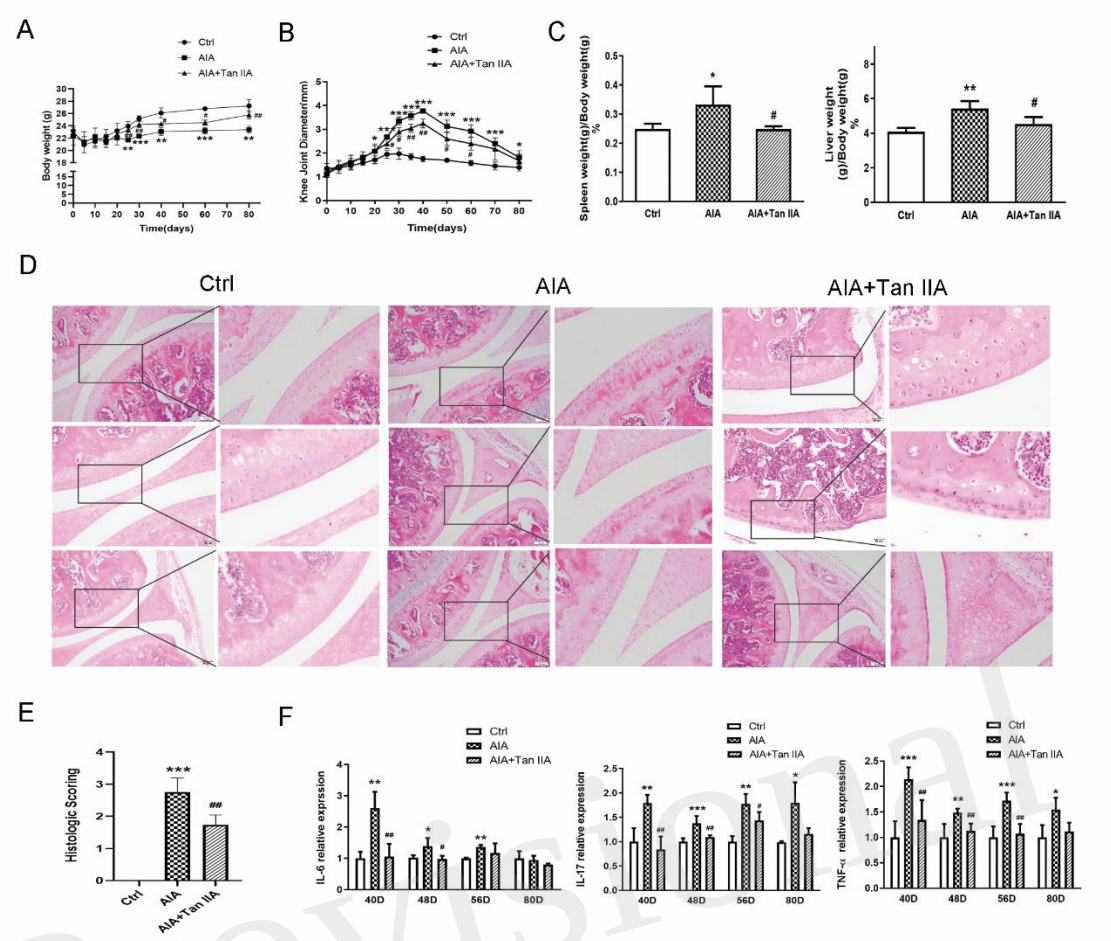


917

918

919 **Fig.3**

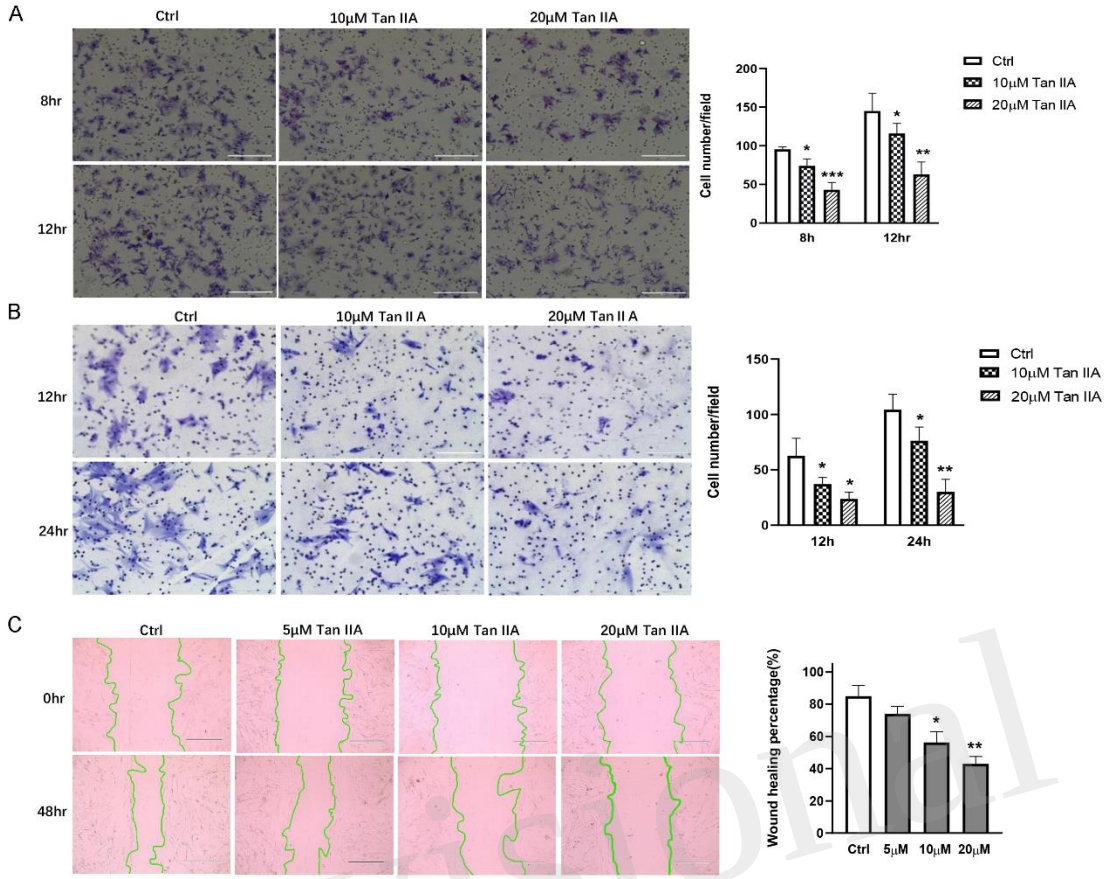


920

921 **Fig. 4**

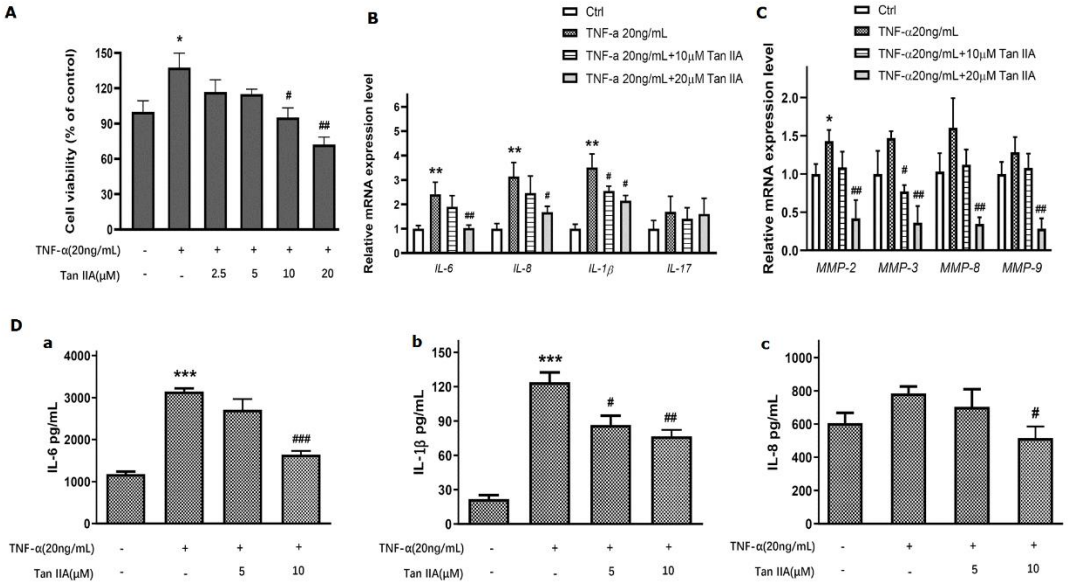


922

923 **Fig. 5**

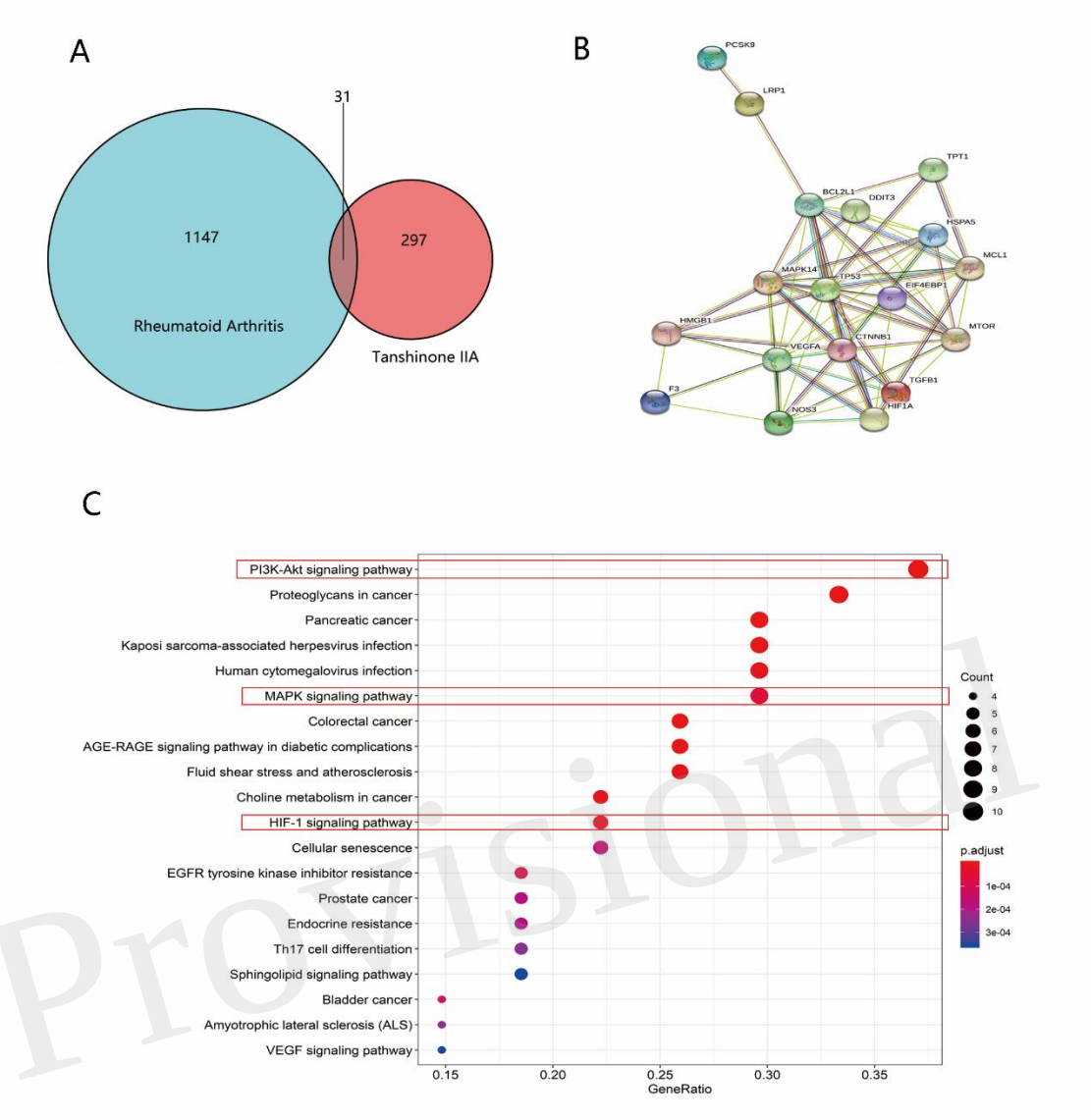


924

925

926 **Fig. 6**

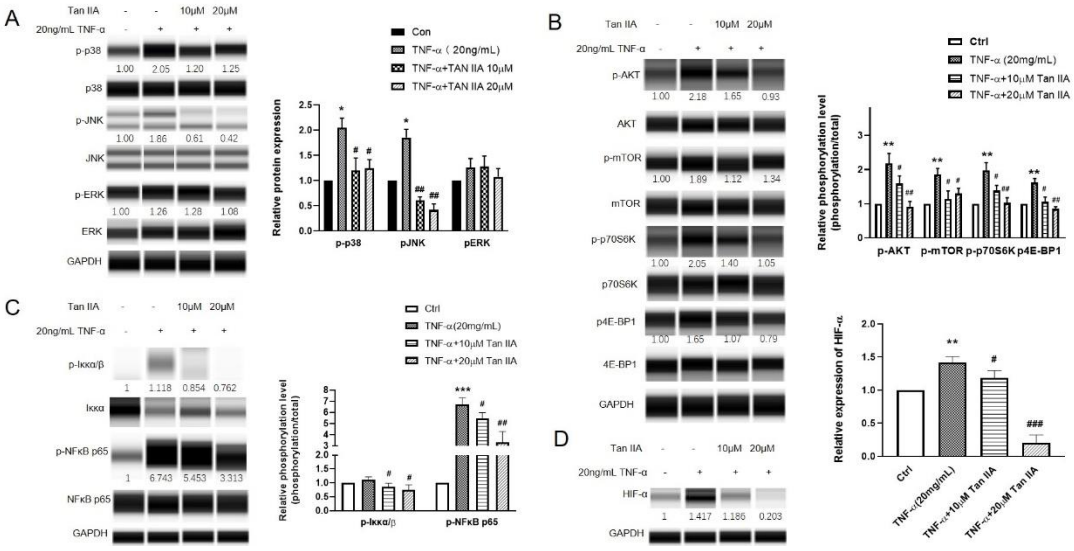


927

928

## SUPPLEMENTARY MATERIAL

### Table S1. The information of RA patients whose tissue samples were used in our research

| NO. OF PATIENTS | GENDER | AGE | RF (IU/ML) | ESR | C-REACTIN PROTEIN (MG/L) | ACPA |
|---|---|---|---|---|---|---|
| **1** | FEMALE | 60 | 4760 | 60 | 127 | Positive |
| **2** | FEMALE | 61 | 795 | 23 | 109 | Positive |
| **3** | MALE | 55 | 948 | 103 | 85.3 | Positive |
| **4** | FEMALE | 24 | 678 | 90 | 45.9 | Positive |
| **5** | FEMALE | 60 | 202 | 56 | <3.14 | Positive |
| **6** | MALE | 57 | 998 | 29 | 28.6 | Positive |

All the patients removed synovial tissues in our research were not treated with biologics or JAK inhibitors.

Remark: Rheumatoid factor (RF); Erythrocyte sedimentati on rate (ESR); Anti-cyclic citrullinated peptide antibodies(ACPA)

938 **Table S2.The primers of human cytokines and MMPs**

939 **for mRNA expression assay**

940

| GENE NAME | | SEQUENCE | NUMBER OF BASES(BPS) |
|---|---|---|---|
| **IL-6** | Forward | AGTGAGGAACAAGCCAGAGC | 20 |
| | Reverse | AGCTGCGCAGAATGAGATGA | 20 |
| **IL-8** | Forward | AGAAGTTTTTGAAGAGGGCTGAGA | 25 |
| | Reverse | AGTTTCACTGGCATCTTCACTGATT | 25 |
| **IL-1B** | Forward | CCACCTCCAGGGACAGGATA | 20 |
| | Reverse | AACACGCAGGACAGGTACAG | 20 |
| **IL-17** | Forward | CTGTCCCCATCCAGCAAGAG | 20 |
| | Reverse | AGGCCACATGGTGGACAATC | 20 |
| **MMP-2** | Forward | TCGCCCATCATCAAGTTCCC | 20 |
| | Reverse | GGGCAGCCATAGAAGGTGTT | 20 |
| **MMP-3** | Forward | TCCGACACTCTGGAGGTGAT | 20 |
| | Reverse | ACTTCGGGATGCCAGGAAAG | 20 |
| **MMP-8** | Forward | ATGTGACGGGGAAGCCAAAT | 20 |
| | Reverse | AAAACCACCACTGTCAGGCA | 20 |
| **MMP-9** | Forward | GGACAAGCTCTTCGGCTTCT | 20 |
| | Reverse | TCGCTGGTACAGGTCGAGTA | 20 |

941

942

943

Figure 01.TIF



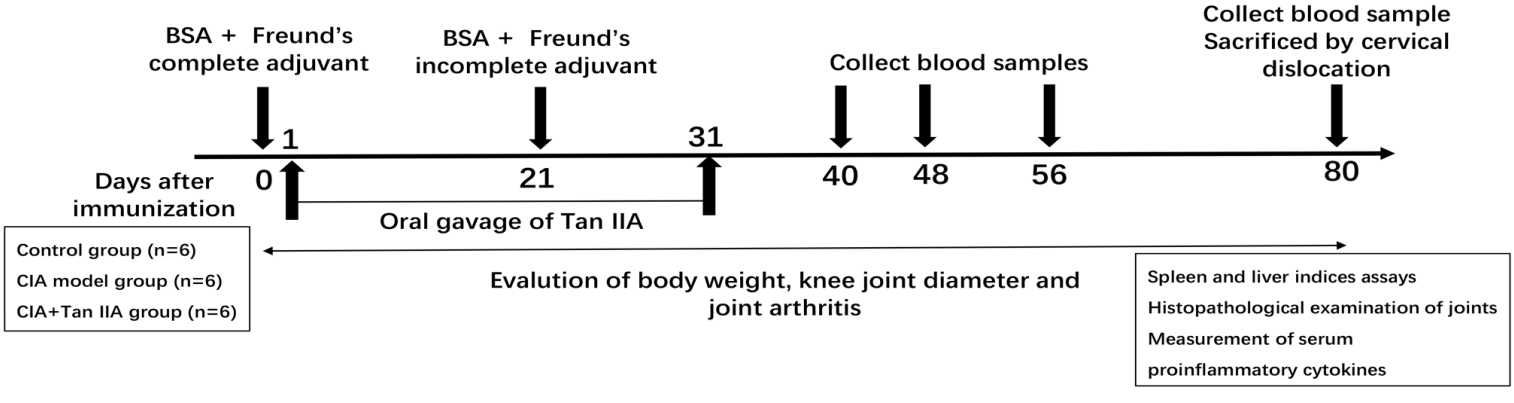

Figure 02.TIF

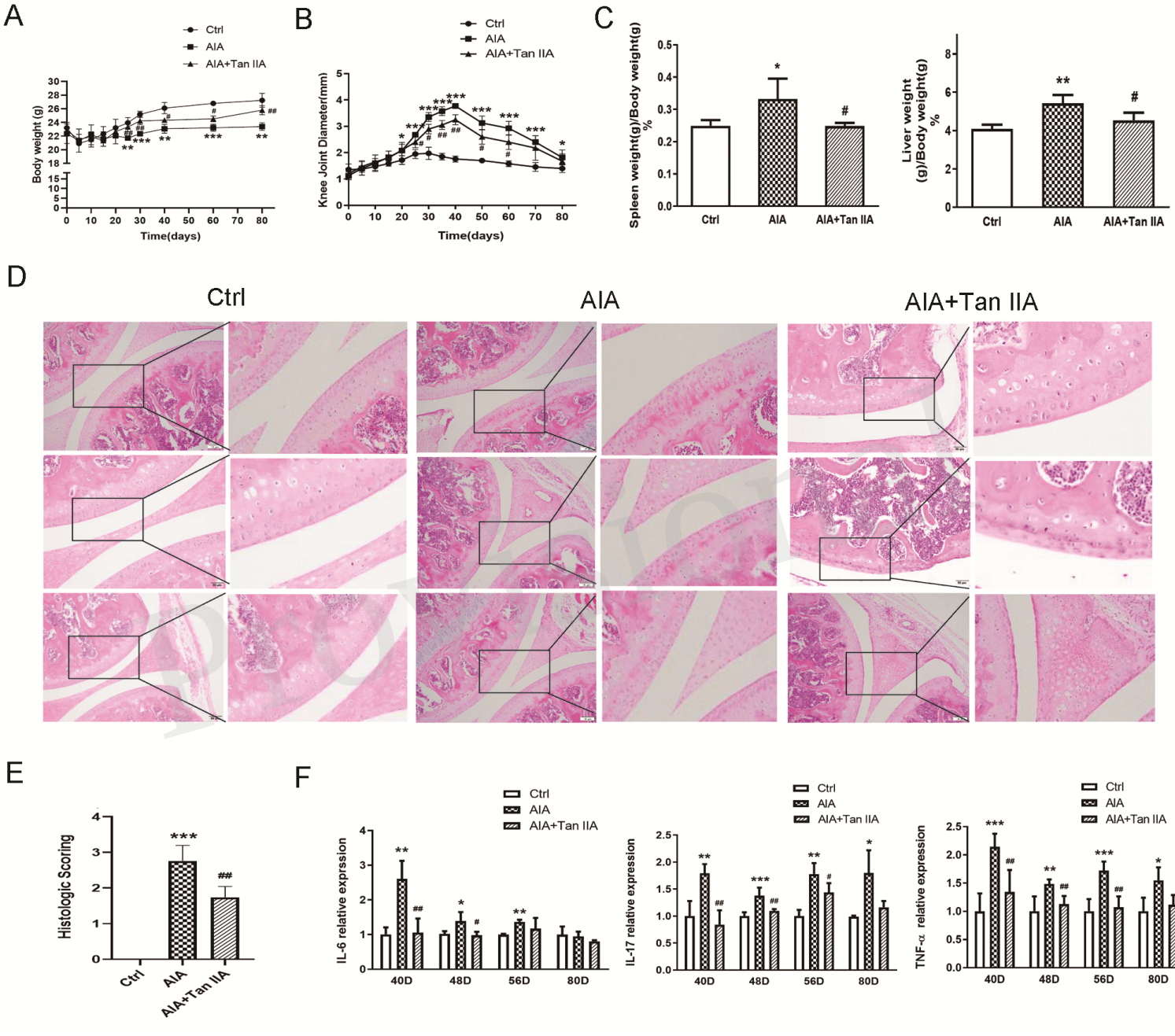

Figure 03.TIF

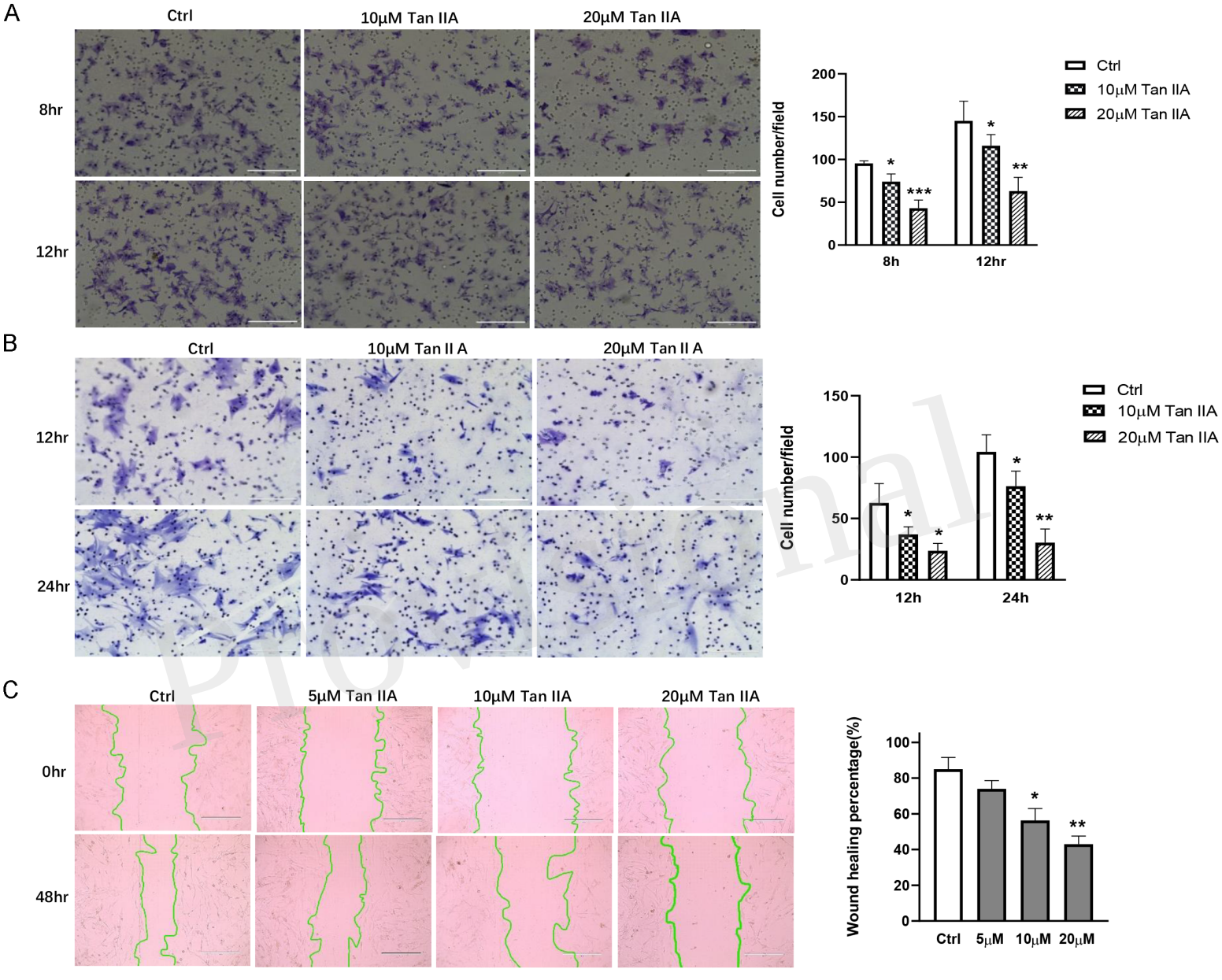

Figure 04.TIF

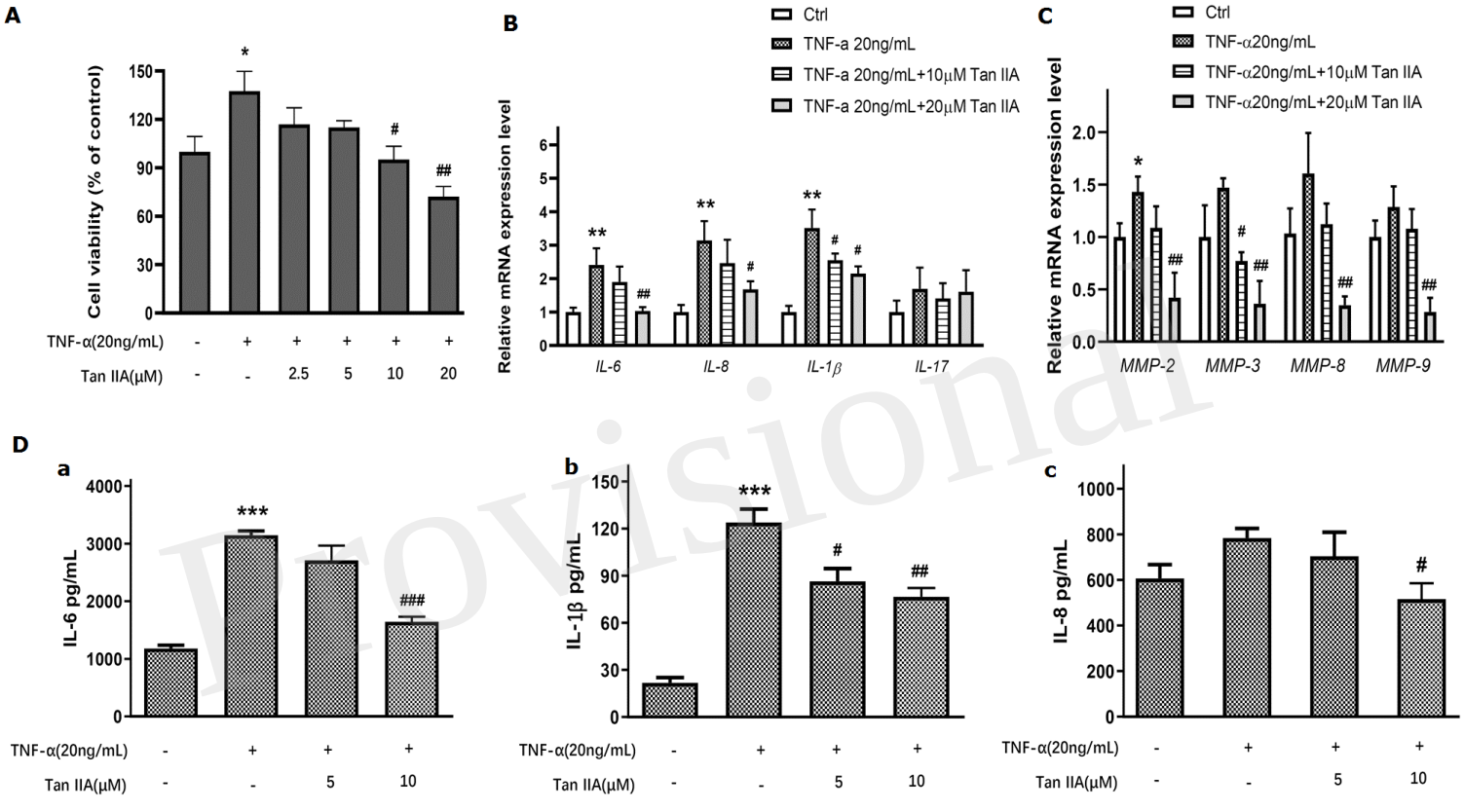

Figure 05.TIF

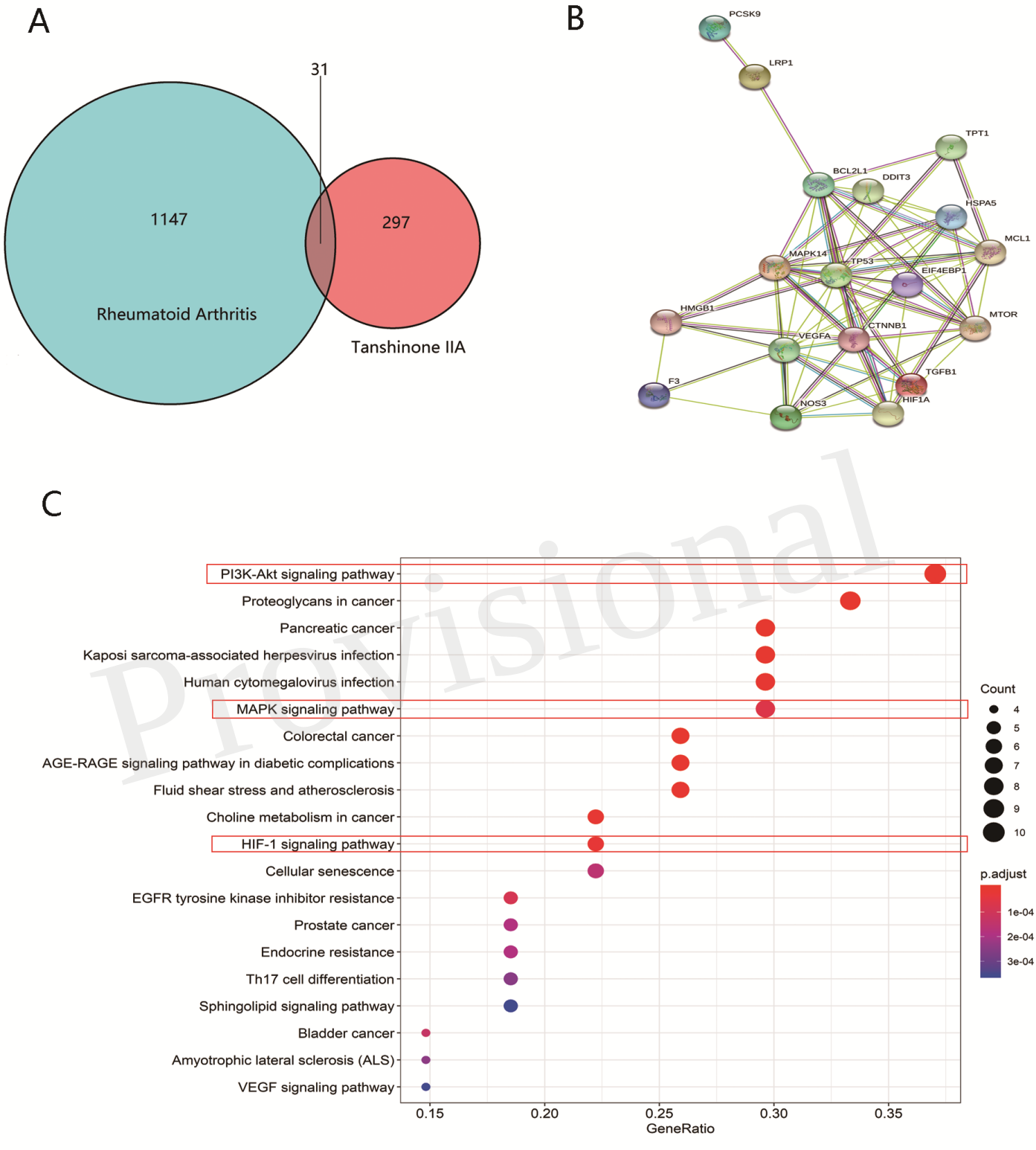

Figure 06.JPEG